

Adiabatic regularization of power spectrum and stress tensor of relic gravitational wave without low-frequency distortion

Yang Zhang*, Bo Wang †

Department of Astronomy, Key Laboratory for Researches in Galaxies and Cosmology,
University of Science and Technology of China,
No.96, JinZhai Road, Hefei, Anhui, 230026, China

Abstract

Adiabatic regularization is a method to remove UV divergences in quantum fields in curved spacetime. For relic gravitational wave generated during inflation, regularization on all k -modes of the power spectrum to 2nd adiabatic order, and of the energy density and pressure to 4th order, respectively, causes low-frequency distortions. To avoid these, we regularize only the short modes inside the horizon during inflation (corresponding to the present frequencies $f \gtrsim 10^9 \text{Hz}$), and keep the long modes intact. Doing this does not violate the energy conservation since the k -modes of RGW are independent of each other during inflation. The resulting spectra are UV convergent and simultaneously free of low-frequency distortion, and these properties remain in the present spectra after evolution, in contrast to regularization at the present time which has some distortion or irregularities. The spectra generally exhibit quick oscillations in frequency domain, even if the initial spectra during inflation have no oscillations. This pattern is due to the interference between the positive and negative frequency modes developed during cosmic expansion, and may be probed by future RGW detections.

PACS numbers: 04.62.+v, 04.30.-w, 98.80.Cq

Quantum fields in curved spacetime, Gravitational waves, inflationary universe,

1 Introduction

Quantum fields in Minkowski spacetime have ultra-violet (UV) divergences, such as the zero-point energy of an infinite number of k -modes of the vacuum fluctuations. This UV divergence is usually removed by the procedure of normal ordering, which amounts to drop the vacuum fluctuations as a whole. This practice is justified in flat spacetime since gravitational effects of the vacuum energy are not considered. In Robertson-Walker spacetime quantum fields also contain the UV divergence of vacuum fluctuations, and one has to treat it with care, because the finite part of the vacuum fluctuations has important physical effects in curved spacetime [1]. For instance, the vacuum fluctuations of metric perturbations during inflation are the origin of cosmological perturbations, and induce

*yzh@ustc.edu.cn

†ymwangbo@mail.ustc.edu.cn

CMB anisotropies and polarization. While scalar metric perturbation serves as the seed for large scale structure formation, the tensor perturbation forms a stochastic background of relic gravitational wave (RGW) [2–10]. It has a very broad power spectrum covering the bands of almost all the current GW detectors. In particular, its high frequency part ($f \gtrsim 10^9 \text{Hz}$) is the target of the high-frequency Gaussian beam detectors [11, 12]. RGW during inflation is a quantum field, the power spectrum defined in the vacuum state has UV divergences, which must be removed. The adiabatic regularization [13–18] is useful in removing UV divergences in the k -modes of quantum fields. Refs. [18, 19] applied to a scalar field during inflation, found that the power spectrum is changed at lower frequency.

Ref. [20] suggested that, for the far low frequency at the end of inflation, no adiabatic subtraction should be performed. Ref. [21] argued that the adiabatic regularization is not valid for the modes after the horizon exit. Ref. [22] showed that the counter term of regularization becomes negligibly small after the Hubble radius crossing, so that the regularized power spectrum tends to the unregularized one. Refs. [23–25] confirmed this by some inflation models. Refs. [26, 27] pointed out that a prescription of adiabatic regularization is not unique from perspective of renormalization, because the infinities to be absorbed into the bare constants can always carry along a finite term, and each different finite term will correspond to a different scheme of adiabatic regularization. In our previous work [28] (as Paper I), we studied adiabatic regularization on RGW, and examined three prescriptions of regularization of power spectrum as well as the stress tensor, but the low-frequency distortions were not addressed in details.

The infrared (IR) band ($10^{-20} \sim 10^{-15} \text{Hz}$) of the power spectrum is related to the spectra C_l^{XX} at $l = (2 \sim 3000)$ of CMB anisotropies and polarization [29–32], any distortion in this band will affect the predicted C_l^{XX} . Moreover, as we shall see, the IR convergence of spectra can be even altered by the all- k regularization. Therefore, it is would be desired that the low frequency portion remains intact under the adiabatic regularization, since its original aim is to remove only UV divergences. So the scheme to carry out regularization has to be carefully constructed.

In this paper, we shall present a detailed study of the low-frequency distortions brought about by all- k regularization upon the power spectrum, and the stress tensor of RGW. We shall trace the origin of distortions, and make a distinction that only the inside-horizon modes are responsible for UV divergences, whereas the outside-horizon modes contain no UV divergences. So we shall naturally regularize only these high-frequency modes, and hold the low frequency modes intact. This inside-horizon scheme of regularization is legitimate because, at the level of the linearized Einstein equation, the k -modes of RGW are independent of each other. The resulting regularized spectra are UV convergent and free of low-frequency distortions as well. With these as the initial condition, the evolution will yield the present spectra which are well-behaved. We shall also examine other possible schemes of regularization performed at the present stage, and compare them. We shall analyze the structure of RGW as a quantum field at present stage as a result of evolution from inflation, particularly demonstrate the oscillatory pattern due to interference between the positive and negative frequency modes. The paper is organized as follows.

In Sect. 2, we introduce the analytical solution of RGW, and analyze the UV and IR asymptotic behaviors of the power spectrum, the spectral energy density and pressure.

In Sect. 3, we examine the all- k adiabatic regularization of the spectra during inflation, and demonstrate the low-frequency distortions and the occurrence of IR divergences.

In Sect. 4, we remedy this by the scheme of inside-horizon regularization during inflation.

In Sect. 5, we let the initial regularized spectra of Sect.4 evolve into the present spectra.

In Sect. 6, we analyze the structure of RGW at the present stage, demonstrate the oscillatory pattern in the spectra due to the interference.

In Sect. 7, we examine possible regularization at the present time, and compare with those in Sect. 5.

Sect. 8 contains the conclusions and discussions.

Appendix A gives the adiabatic counter terms, Appendix B gives the asymptotic expressions of modes at high frequency, Appendix C lists the analytical RGW solution from inflation up to the present accelerating stage.

We use the unit with $c = \hbar = 1$ in this paper.

2 Power spectrum, energy density, pressure of RGW

The metric of a flat Robertson-Walker spacetime is written as

$$ds^2 = a^2(\tau)[d\tau^2 - (\delta_{ij} + h_{ij})dx^i dx^j], \quad (2.1)$$

in synchronous gauge, where τ is the conformal time, and h_{ij} is traceless and transverse RGW. To linear order, the wave equation is $\square h_{ij} = 0$. As a quantum field, it is written as

$$h_{ij}(\mathbf{x}, \tau) = \int \frac{d^3k}{(2\pi)^{3/2}} \sum_{s=+, \times} \epsilon_{ij}^s(k) \left[a_{\mathbf{k}}^s h_k^s(\tau) e^{i\mathbf{k}\cdot\mathbf{x}} + a_{\mathbf{k}}^{s\dagger} h_k^{s*}(\tau) e^{-i\mathbf{k}\cdot\mathbf{x}} \right], \quad (2.2)$$

where $k = |\mathbf{k}|$ is the comoving wavenumber, two polarization tensors satisfy

$$\epsilon_{ij}^s(k) \delta_{ij} = 0, \quad \epsilon_{ij}^s(k) k^i = 0, \quad \epsilon^{ij}(k) \epsilon_{ij}^{s'}(k) = \delta_{ss'}, \quad (2.3)$$

and $a_{\mathbf{k}}^s$ and $a_{\mathbf{k}}^{s\dagger}$ are the annihilation and creation operators of graviton satisfying the canonical commutation relation

$$\left[a_{\mathbf{k}}^s, a_{\mathbf{k}'}^{r\dagger} \right] = \delta_{sr} \delta^3(\mathbf{k} - \mathbf{k}'). \quad (2.4)$$

For RGW, the two polarization modes h_k^+ and h_k^\times are assumed to be independent and statistically equivalent, so that the superscript $s = +, \times$ can be dropped. The k -mode equation is

$$h_k''(\tau) + 2 \frac{a'(\tau)}{a(\tau)} h_k'(\tau) + k^2 h_k(\tau) = 0. \quad (2.5)$$

The second order RGW [33,34] is not considered here. We emphasize that, at the level of first order metric perturbations, the RGW equation is homogeneous, and these k -modes of RGW are *independent*, as they do not couple to each other, and no energy exchanges between different k -modes. Consequently, from statistical perspective, the modes h_k can be described by a Gaussian process, the mean is zero and the variance is given by its power spectrum that we shall calculate soon. Let

$$h_k(\tau) \equiv \frac{A}{a(\tau)} u_k(\tau), \quad (2.6)$$

where $A \equiv \sqrt{32\pi G} = \frac{2}{M_{Pl}}$ with $M_{Pl} \equiv 1/\sqrt{8\pi G}$ being the Planck mass, determined by the quantum normalization that there is a zero point energy $\frac{1}{2}\hbar\omega$ in high frequency limit in each \mathbf{k} -mode and each polarization of RGW. The mode u_k satisfies the wave equation

$$u_k''(\tau) + \left[k^2 - \frac{a''(\tau)}{a(\tau)} \right] u_k(\tau) = 0. \quad (2.7)$$

For each stage of cosmic expansion, i.e., inflation, reheating, radiation dominant, matter dominant and the present accelerating, the scale factor is taken as a power-law form $a(\tau) \propto \tau^b$ where b is a constant, and the exact solution of Eq.(2.7) is a combination of Hankel functions,

$$u_k(\tau) = \sqrt{\frac{\pi}{2}} \sqrt{\frac{\sigma}{2k}} [C_1 H_{b-\frac{1}{2}}^{(1)}(\sigma) + C_2 H_{b-\frac{1}{2}}^{(2)}(\sigma)], \quad (2.8)$$

where $\sigma \equiv k\tau$, and C_1, C_2 are coefficients determined by continuity of u_k, u_k' at the transition of two consecutive stages. Thus, the analytical solution $h_k(\tau)$ is obtained for the whole course of evolution [9, 10]. Appendix C gives the coefficients for these five expanding stages by connecting the adjoining stages. For the inflation, one has

$$a(\tau) = l_0 |\tau|^{1+\beta}, \quad -\infty < \tau \leq \tau_1, \quad (2.9)$$

where two constants l_0 and β are the parameters of the model, τ_1 is the ending time of inflation [5, 6, 9, 10]. For various values of the index $\beta \sim -2$, the scale factor in (2.9) describes a class of inflation models. The expansion index β is related to the slow-roll parameter ϵ of inflation via $\beta = \frac{-2+\epsilon}{1-\epsilon}$. In de Sitter inflation, $\beta = -2$, $l_0^{-1} = H$ is the inflation expansion rate. Eq.(2.7) has a general solution

$$u_k(\tau) = \sqrt{\frac{\pi}{2}} \sqrt{\frac{x}{2k}} [A_1 e^{i\pi(\beta+1)/2} H_{\beta+\frac{1}{2}}^{(1)}(x) + A_2 e^{-i\pi(\beta+1)/2} H_{\beta+\frac{1}{2}}^{(2)}(x)], \quad (2.10)$$

$$-\infty < \tau \leq \tau_1,$$

where $x \equiv |k\tau| = -k\tau$, the phase $e^{-i\pi(\beta+1)/2}$ is chosen for simplicity at high frequency. Each choice of k -dependent coefficients (A_1, A_2) defines a choice of quantum state of RGW during inflation. The Wronskian as a conserved quantity

$$u_k(\tau)u_k'^*(\tau) - u_k^*(\tau)u_k'(\tau) = i \quad (2.11)$$

is required for the modes u_k and u_k^* as the two independent of solutions of the wave equation, and it is checked by using $H_k^{(1)} \frac{d}{dx} H_k^{(2)} - H_k^{(2)} \frac{d}{dx} H_k^{(1)} = -\frac{4i}{\pi x}$. The Wronskian (2.11) holds also in other expansion stages when the mode and its derivative are connected continuously. Application of (2.11) to the mode solution (2.10) gives a relation $|A_2|^2 - |A_1|^2 = 1$. By $H_{\beta+\frac{1}{2}}^{(1)} = H_{\beta+\frac{1}{2}}^{(2)*}$, the solution (2.10) can be denoted by

$$u_k(\tau) = A_1 v_k^*(\tau) + A_2 v_k(\tau), \quad (2.12)$$

where

$$v_k(\tau) \equiv \sqrt{\frac{\pi}{2}} \sqrt{\frac{x}{2k}} e^{-i\pi \frac{(\beta+1)}{2}} H_{\beta+\frac{1}{2}}^{(2)}(x). \quad (2.13)$$

In high frequency limit $k \rightarrow \infty$, it approaches to

$$v_k \rightarrow \frac{e^{-ik\tau}}{\sqrt{2k}} \left(1 - i \frac{\beta(\beta+1)}{2k\tau} - \frac{(\beta+2)(\beta+1)\beta(\beta-1)}{8k^2\tau^2} + \mathcal{O}(k^{-3}) \right), \quad (2.14)$$

where the leading term $\frac{e^{-ik\tau}}{\sqrt{2k}}$ is identified as the positive-frequency vacuum mode in Minkowski spacetime, and other terms reflect the effects of the expanding RW spacetime. (See (B.6) in Appendix B.) The conjugate v^* in (2.12) is associated with the negative-frequency mode. In general, the solution (2.10) contains both positive and negative frequency modes, and the mode h_k is written as

$$h_k(\tau) = \frac{H\sqrt{\pi}}{M_{Pl}} |\tau|^{-\beta-\frac{1}{2}} \left[A_1 e^{i\pi(\beta+1)/2} H_{\beta+\frac{1}{2}}^{(1)}(x) + A_2 e^{-i\pi(\beta+1)/2} H_{\beta+\frac{1}{2}}^{(2)}(x) \right], \quad (2.15)$$

for $-\infty < \tau \leq \tau_1$.

One sees that its amplitude during inflation is mainly determined by the ratio H/M_{Pl} .

We work in Heisenberg picture, in which RGW as a quantum field operator evolves in time, whereas Fock space vector of quantum state does not change with time. One defines the vacuum state vector $|0\rangle$ such that

$$a_{\mathbf{k}}^s |0\rangle = 0, \quad \text{for all } \mathbf{k}, \text{ and } s = +, \times. \quad (2.16)$$

The power spectrum of RGW is defined by

$$\int_0^\infty \Delta_t^2(k, \tau) \frac{dk}{k} \equiv \langle 0 | h^{ij}(\mathbf{x}, \tau) h_{ij}(\mathbf{x}, \tau) | 0 \rangle, \quad (2.17)$$

where the vacuum expectation value

$$\langle 0 | h^{ij}(\mathbf{x}, \tau) h_{ij}(\mathbf{x}, \tau) | 0 \rangle = \frac{1}{(2\pi)^3} \int d^3k (|h_k^+|^2 + |h_k^\times|^2), \quad (2.18)$$

is the auto-correlation function of RGW. One reads off the spectrum

$$\Delta_t^2(k, \tau) = 2 \frac{k^3}{2\pi^2} |h_k(\tau)|^2 = \frac{k^3}{\pi^2 a^2} \frac{4}{M_{Pl}^2} |u_k(\tau)|^2, \quad (2.19)$$

where the factor 2 is from the two polarizations $+, \times$. The definition (2.18) applies to any stage of cosmic expansion. When the choice

$$A_1 = 0, \quad A_2 = 1, \quad (2.20)$$

is taken for inflation, the mode $u_k = v_k$, the state defined by (2.16) is called the Bunch-Davies vacuum. This specifies an initial condition of RGW during inflation which is used in this paper, and the power spectrum during inflation becomes

$$\Delta_t^2(k, \tau) = \frac{k^3}{\pi^2 a^2 M_{Pl}^2} |v_k(\tau)|^2 = \frac{k^{2(\beta+2)}}{\pi l_0^2 M_{Pl}^2} x^{-(2\beta+1)} |H_{\beta+\frac{1}{2}}^{(2)}(x)|^2, \quad (2.21)$$

which holds for any time τ during inflation. For the de Sitter inflation $\beta = -2$, $v_k = \frac{1}{\sqrt{2k}} \left(1 - \frac{i}{x} \right) e^{-ix}$, (2.21) reduces to

$$\Delta_t^2(k, \tau) = \frac{2k^2}{\pi^2 M_{Pl}^2 a^2(\tau)} \left(1 + \frac{1}{(k\tau)^2} \right). \quad (2.22)$$

In the long wavelength limit $x \ll 1$, (2.21) becomes the primordial spectrum of RWG

$$\Delta_t^2(k, \tau) \simeq a_t^2 \frac{2}{\pi^2} \left(\frac{H}{M_{Pl}} \right)^2 k^{2\beta+4} \propto k^{2\beta+4} \quad (2.23)$$

with $a_t \simeq 1.01$ for $\beta = -2.02$, which is often written as [37–39]

$$\Delta_t^2(k) = \Delta_R^2 r \left(\frac{k}{k_0} \right)^{n_t + \frac{1}{2}\alpha_t \ln(\frac{k}{k_0})}, \quad (2.24)$$

with the pivot wavenumber $k_0 = 0.002 \text{Mpc}^{-1}$ for WMAP. In our model there are relations $n_t = 2\beta + 4$ and $n_t = n_s - 1$ [28]. The observed value of the scalar spectral index $n_s = 0.962 \sim 0.972$ gives $\beta \simeq -2.019 \sim -2.014$. For demonstration purpose, we shall take $\beta = -2.02$ and $\beta = -1.98$. The scalar curvature spectrum $\Delta_R^2 \simeq 2.47 \times 10^{-9}$ and the tensor-scalar ratio $r < 0.11$ [35, 36]. This leads to an upper limit $\frac{2}{\pi^2} \left(\frac{H}{M_{Pl}} \right)^2 < 2.4 \times 10^{-10}$, i.e., $H < 3.6 \times 10^{14} \text{GeV}$. To be specific, we take $H \sim 3 \times 10^{14} \text{GeV}$, corresponding to an inflation energy scale $\rho^{1/4} \sim 3.5 \times 10^{16} \text{GeV}$.

The frequency at time τ is related to k via $f(\tau) = k/2\pi a(\tau)$. By the normalization of $a(\tau)$ adopted in this paper, the present frequency is

$$f \simeq 1.7 \times 10^{-19} k \text{ Hz}. \quad (2.25)$$

In particular, the conformal wavenumber k of horizon-crossing at the end of inflation is $k \simeq 1/|\tau_1|$, which corresponds to $f = \frac{a(\tau_1)}{a(\tau_H)} \frac{H}{2\pi}$. Using $H \sim 3 \times 10^{14} \text{GeV}$ and $\frac{a(\tau_H)}{a(\tau_1)} \sim 7 \times 10^{28}$ gives $f \simeq 10^9 \text{Hz}$. It should be mentioned that Paper I [28] adopted $f \sim 10^{11} \text{Hz}$ based on a longer reheating model.

If $\Delta_t^2 \propto k^d$ for $d \geq 0$ at high frequencies, the auto-correlation (2.17) will have UV divergence coming from the upper limit of integration. During inflation the squared absolute mode $|v_k|^2 \propto k^{-1}, k^{-3}$ at high frequency (see (B.7)), so that the UV behavior of the spectrum is the following

$$\Delta_t^2 \propto k^2, k^0,$$

where k^2 is the quadratic UV divergence coming from the Minkowski spacetime modes $\frac{e^{-ik\tau}}{\sqrt{2k}}$ of (2.14), and k^0 is the logarithmic UV divergence which exists in a RW spacetime. These UV divergences are to be removed by adiabatic regularization.

The IR behavior of the spectrum as $k \rightarrow 0$ is sensitive to the index β , as indicated by Eq.(2.23). For $\beta < -2$ models which are favored by CMB observations, the auto-correlation at the lower limit $k = 0$ of integration is proportional to the following

$$\int_0 k^{2\beta+4} \frac{dk}{k} = \infty, \quad (2.26)$$

i.e., the auto-correlation is IR power divergent. For $\beta = -2$ de Sitter inflation, $\Delta_t^2 \propto k^0$, the lower limit gives $\propto \int_0 \frac{dk}{k} = -\ln k|_0 = \infty$, the correlation is logarithmically IR divergent. For $\beta > -2$, $\Delta_t^2 \rightarrow 0$ at $k = 0$, and the correlation is IR convergent. Ideally, an adiabatic regularization procedure should not alter the IR behaviors, or at least, should not make an IR convergent spectrum into IR divergent. Nevertheless, as we shall see, this can happen for certain inflation models.

We examine the UV and IR behaviors of the energy density and pressure of RGW. There are several definitions of energy-momentum tensor of RGW arising from different considerations [2, 40–48]. For specific, we consider the following one [28, 40–44]

$$t_{\mu\nu} = \frac{1}{32\pi G} \langle 0 | h^{ij}_{, \mu} h_{ij, \nu} | 0 \rangle, \quad (2.27)$$

which belongs to the effective stress tensor, and is not covariantly conserved by itself. The total energy-momentum tensor is covariantly conserved, including RGW and other matter components as well [41–45, 47]. The RGW energy density is

$$\rho_{gw} = t^0{}_0 = \frac{1}{32\pi G a^2} \int \frac{d^3 k}{(2\pi)^3} 2 |h'_k(\tau)|^2 = \int_0^\infty \rho_k(\tau) \frac{dk}{k}, \quad (2.28)$$

with the spectral energy density

$$\rho_k(\tau) = \frac{k^3}{\pi^2 a^2} \left| \left(\frac{u_k}{a} \right)' \right|^2, \quad (2.29)$$

the RGW pressure is given by

$$p_{gw} = -\frac{1}{3} t^i{}_i = \frac{1}{96 a^2 \pi G} \int \frac{d^3 k}{(2\pi)^3} 2 k^2 |h_k|^2 = \int_0^\infty p_k(\tau) \frac{dk}{k}, \quad (2.30)$$

with the spectral pressure

$$p_k(\tau) = \frac{k^5}{3\pi^2 a^4} |u_k(\tau)|^2. \quad (2.31)$$

Other definitions of ρ_k and p_k of RGW also involve linear combinations of $|u_k|^2$ and $\left| \left(\frac{u_k}{a} \right)' \right|^2$ as an essential part.

For de Sitter inflation, by (B.7) (B.9), the spectral energy density and pressure have the following simple expressions

$$\rho_k(\tau) = \frac{k^3}{\pi^2 a^2} \frac{k}{2a^2} = \frac{k^4}{2\pi^2 a^4}, \quad (2.32)$$

$$p_k(\tau) = \frac{k^5}{3\pi^2 a^4} |v_k(\tau)|^2 = \frac{k^4}{6\pi^2 a^4} \left(1 + \frac{1}{(k\tau)^2} \right). \quad (2.33)$$

Note that $\rho'_k + 3 \frac{a'}{a} (\rho_k + p_k) = \frac{a'}{a} \frac{1}{x^2} \rho_k \neq 0$ since the effective $t_{\mu\nu}$ is not covariantly conserved, as mentioned earlier. In high frequency limit, both ρ_k and p_k are UV divergent, and in low frequency limit, $\rho_k \propto H^4 k^4$ and $p_k \propto H^4 k^2$, both are IR convergent. For general $\beta \sim -2$ models, in high frequency limit, by (B.7) (B.9),

$$\rho_k \simeq \frac{k^4}{2\pi^2 a^4}, \quad p_k \simeq \frac{k^4}{2\pi^2 a^4}. \quad (2.34)$$

In low frequency limit,

$$|v_k|^2 \simeq b_t k^{-1} x^{2\beta+2}, \quad \left| \left(\frac{v_k}{a} \right)' \right|^2 \simeq c_t l_0^{-2} |\tau|^2 k^{2\beta+5},$$

where $b_t \equiv \frac{\sin(\pi\beta)^2\Gamma(-\beta-\frac{1}{2})^2\Gamma(\beta+\frac{3}{2})^2+\pi^2}{\pi^{2\beta+3}\Gamma(\beta+\frac{3}{2})^2} \simeq \frac{1}{2}$, $c_t \equiv \frac{\sin(\pi\beta)^2\Gamma(-\beta-\frac{1}{2})^2\Gamma(\beta+\frac{3}{2})^2+\pi^2}{\pi^{2\beta+3}(2\beta+3)^2\Gamma(\beta+\frac{3}{2})^2} \simeq \frac{1}{2}$, so

$$\rho_k \simeq \frac{c_t}{\pi^2|\tau|^{2\beta}} H^4 k^{2\beta+8} \propto H^4 k^{2\beta+8} \quad \text{for fixed } \tau, \quad (2.35)$$

$$p_k \simeq \frac{b_t}{3\pi^2|\tau|^{2\beta+2}} H^4 k^{2\beta+6} \propto H^4 k^{2\beta+6} \quad \text{for fixed } \tau, \quad (2.36)$$

which are IR convergent. As we shall see, the all- k adiabatic regularization will bring ρ_k , p_k into IR divergent. That is our concern.

3 Adiabatic regularization during inflation

We now analyze in details the occurrence of the low-frequency distortions caused by adiabatic regularization, which was not addressed in Paper I. The UV divergent power spectrum (2.21) changes with time during inflation. At a given instance τ , the spectrum approximately is flat $\propto k^{2\beta+4} \sim k^0$ for $k \lesssim 1/|\tau|$ (except at the IR end $k \sim 0$), and rises up as $\propto k^2$ for $k \gtrsim 1/|\tau|$, i.e., the horizon-crossing $k|\tau| = 1$ is the point where the spectrum starts to rise up. By examining the high-frequency expression of $|v_k(\tau)|^2$ in (B.7), we realize that the point $k|\tau| = 1$ is also where the Minkowski spacetime vacuum term $\frac{1}{2k}$ is roughly equal to the next expansion term $\frac{1}{2k} \frac{\beta(\beta+1)}{2k^2\tau^2}$. The vacuum term is dominant at $k \gtrsim 1/|\tau|$, and the expansion terms are dominant for $k \lesssim 1/|\tau|$. At any time during inflation, the part of vacuum modes which lies inside the horizon causes the k^2 divergence, and the expansion term causes k^0 divergence. The comoving wavenumber of horizon-crossing $k = 1/|\tau|$ corresponds to a present frequency f_τ . For an earlier time, the rising-up frequency f_τ is smaller. Fig.1 (a) illustrates that, at an earlier time $\tau = 1000\tau_1$ the spectrum rises up at $f \sim 10^6\text{Hz}$, and at the end of inflation τ_1 it rises up at $f \sim 10^9\text{Hz}$, respectively. The time $\tau = 1000\tau_1$ is when the scale factor is $a \simeq 10^{-3}a(\tau_1)$.

Given the UV divergences of Δ_i^2 , we subtract them, according to the minimal subtraction rule [13, 18],

$$\Delta_i^2(k, \tau)_{reg} = \frac{A^2 k^3}{\pi^2 a^2(\tau)} \left(|v_k(\tau)|^2 - |v_k^{(2)}(\tau)|^2 \right) \quad \text{for all } k, \quad (3.1)$$

which can apply at a time during inflation instantaneously. We refer to this scheme as the all- k regularization since the subtraction applies for all k -modes simultaneously. $|v_k^{(2)}|^2$ is the counter part of 2nd adiabatic order given by (see (A.17) in Appendix A),

$$|v_k^{(2)}|^2 = \frac{1}{2k} + \frac{(\beta+1)\beta}{4k^3\tau^2}, \quad (3.2)$$

where the first term is to cancel the quadratic divergence from the vacuum modes, and the second term is to cancel the logarithmic divergence. An important property is that during inflation the spectrum regularized at an earlier time will evolve into a spectrum which is regularized at a later time, as illustrated in Fig.1 (b). The regularization (3.1) performed at any time τ during inflation always rightly removes the divergences which rises up at f_τ . (This property is also true in the scheme of inside-horizon regularization in Section 4.) The resulting spectrum after regularization is $\propto k^{-2}$ at high frequency and becomes UV convergent. We show the regularized and unregularized spectrum at the end of inflation

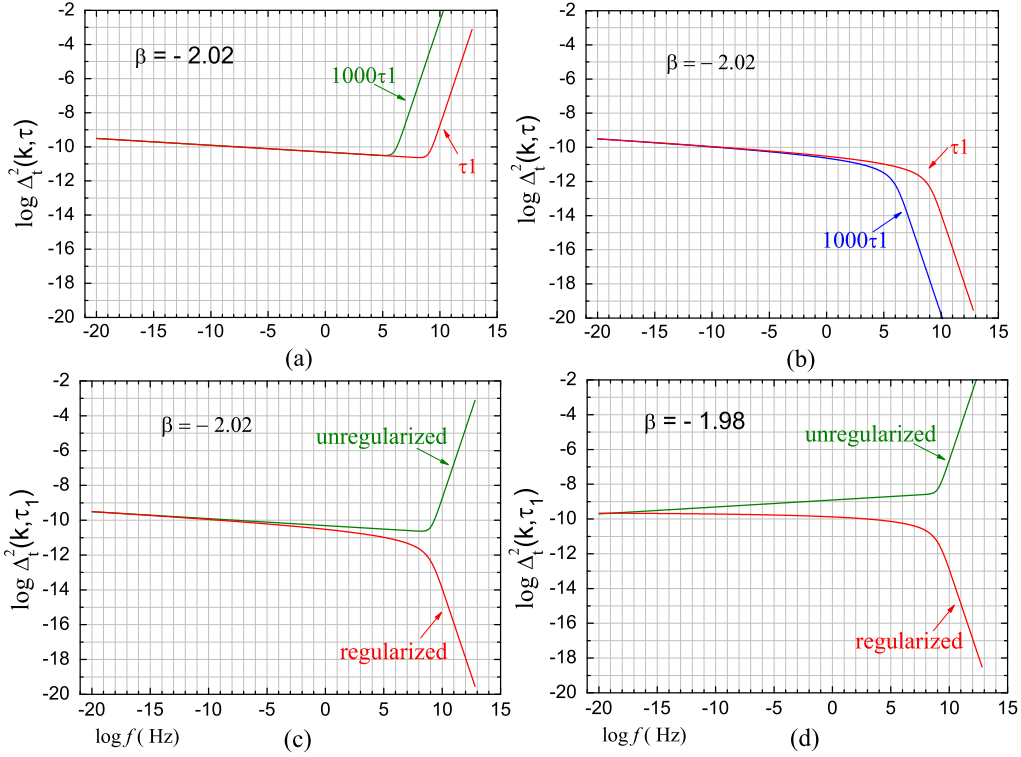


Figure 1: (a) The unregularized power spectrum during inflation. At an earlier time $\tau = 1000\tau_1$ it rises up at $f \sim 10^6$ Hz, at the end of inflation τ_1 it rises up at $f_1 \sim 10^9$ Hz. (b) The spectrum regularized at $1000\tau_1$ and at τ_1 respectively. The former will evolve into the latter. (c) (d) The regularized and unregularized spectrum at τ_1 for the models $\beta = -2.02$ and $\beta = -1.98$. The horizontal axis is converted into the present frequency f by (2.25).

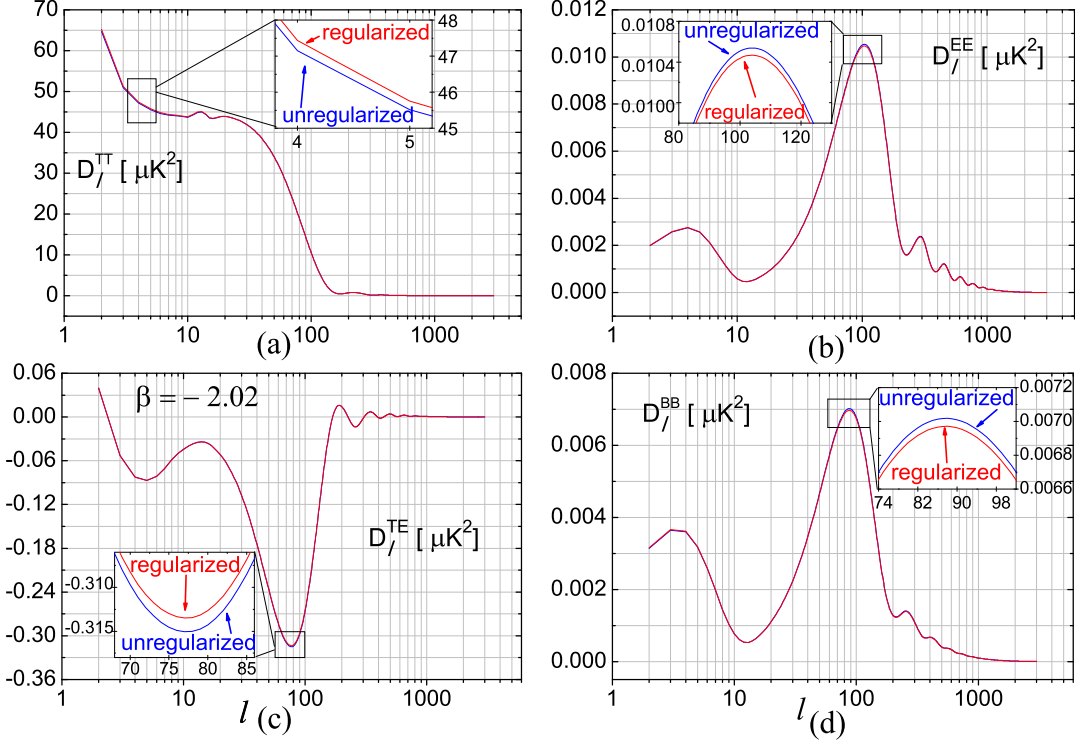


Figure 2: $l(l+1)C_l^{XX}/2\pi$ [μK^2] generated by the regularized and unregularized power spectra of RGW, using CAMB code [49,50]. The difference is tiny.

τ_1 in Fig.1 (c) (d) for the models $\beta = -2.02$ and $\beta = -1.98$, respectively. In the range ($10^{-20} \sim 10^{-15}$)Hz the difference between the regularized and unregularized is rather small ($\sim 0.2\%$). When they are substituted into the integration $C_l^{XX} = \int_{k_{min}}^{k_{max}} \frac{dk}{k} \Delta_t^2(k) P_{Xl}^2(k)$ with P_{Xl}^2 being the projection factors [30,31], they give their respective spectra of CMB anisotropies and polarization. We use CAMB code [49–51] and plot the resulting C_l^{XX} in Fig.2, which show tiny differences. (In computing we have used $k_{min} = 7 \times 10^{-8} \text{Mpc}^{-1}$ and $k_{max} = 0.4 \text{Mpc}^{-1}$, which correspond to the present frequency $f_{min} = 7 \times 10^{-22} \text{Hz}$ and $f_{max} = 0.4 \times 10^{-14} \text{Hz}$. The lower and upper limits of the numerical integration can only take finite values, instead of 0 and ∞ , so that the IR and UV divergences existing in $\Delta_t^2(k)$ are not reflected in the numerical C_l^{XX} .) Nevertheless, in the range ($10^{-9} \sim 10^9$)Hz the regularized power spectrum of RGW has been suppressed considerably by a factor as much as ($1 \sim 10^3$), as seen in Fig.1 (c) and (d). This range covers the working bands of PTA [52–57], LISA [58,59] and LIGO [60]. The suppression is an unwanted outcome of the all- k regularization.

Let us examine the IR behavior of Δ_t^2 at $k \sim 0$ under the regularization. The counterpart at small k gives

$$k^3 \left(\frac{1}{2k} + \frac{(\beta+1)\beta}{4k^3\tau_1^2} \right) \simeq \frac{(\beta+1)\beta}{4\tau_1^2}, \quad (3.3)$$

which is a finite, k -independent constant. So, under the adiabatic subtraction, the all- k regularization will downshift Δ_t^2 at $k \sim 0$ by this constant, and consequently the auto-

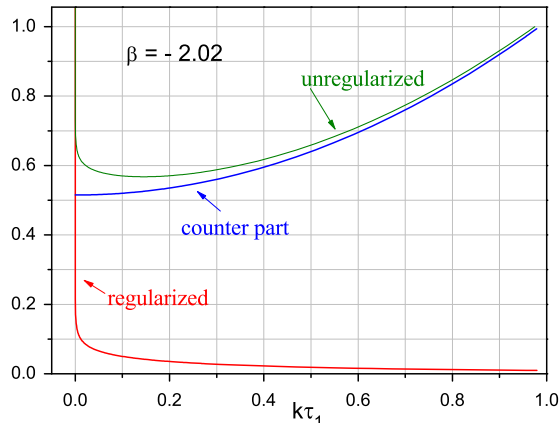


Figure 3: Schematically, Green: the unregularized spectrum is IR divergent and dominant. Blue: the counter part is IR log divergent and subdominant. Red: the regularized spectrum is IR divergent.

correlation will acquire an IR logarithmic divergent term as the following

$$\frac{(\beta + 1)\beta}{4\tau_1^2} \int_0 \frac{dk}{k} = \infty. \quad (3.4)$$

As said early, for the models $\beta < -2$, the unregularized spectrum is already IR power divergent, and the counter term is negligible in the limit $k|\tau| \ll 1$. This case is schematically illustrated in Fig.3, and corresponds to the situation discussed in Refs. [22, 25] when the Hubble parameter at a later time during inflation is smaller than the one at horizon-crossing, $H(\tau)/H(\tau_*) \ll 1$. However, for the models $\beta > -2$, i.e., $H(\tau)/H(\tau_*) > 1$, which Refs. [22, 25] did not consider, the unregularized spectrum is IR convergent, the counter term is IR logarithmic divergent, so that the regularized spectrum is dominated by the counter term and becomes IR logarithmic divergent, as schematically illustrated in Fig.4. Therefore, the all- k regularization has a difficulty for the $\beta > -2$ inflation models, since it makes an IR convergent spectrum into an IR divergent one. It also has a difficulty with the de Sitter inflation, in which the unregularized spectrum (2.22) and the adiabatic counter part (3.2) cancel exactly, yielding a vanishing power spectrum.

More drastic low-frequency distortions are brought about upon the energy density and pressure by the all- k regularization. The energy density and pressure in vacuum contain UV quartic divergence of the 0th order ($\propto k^4$), besides the quadratic divergence of 2nd order ($\propto k^2$) and logarithmic divergence of 4th order ($\propto k^0$). By the minimal subtraction rule, the adiabatic regularization will be applied to the 4th order,

$$\rho_k(\tau)_{reg} = \frac{k^3}{\pi^2 a^2} \left| \left| \left(\frac{v_k(\tau)}{a} \right)' \right|^2 - \left| \left(\frac{v_k^{(4)}(\tau)}{a} \right)' \right|^2 \right|, \quad \text{for all } k, \quad (3.5)$$

where the 4th order counter part during inflation given by (A.15) has the three terms,

$$\left| \left(\frac{v_k^{(4)}(\tau)}{a} \right)' \right|^2 = \frac{1}{a^2} \left[\frac{k}{2} + \frac{(\beta + 1)(\beta + 2)}{4k\tau^2} + \frac{3\beta(\beta + 1)(\beta + 2)(\beta + 3)}{16k^3\tau^4} \right], \quad (3.6)$$

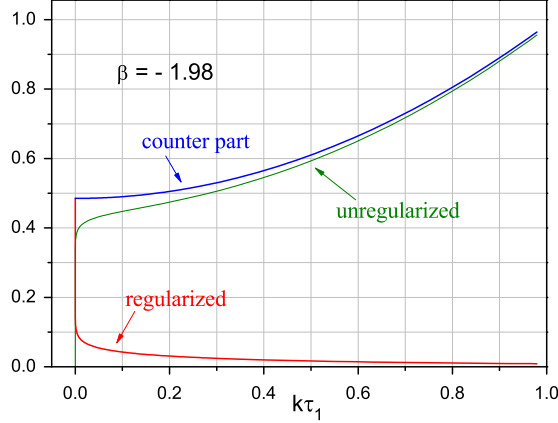


Figure 4: Schematically, Green: the unregularized spectrum is IR convergent and subdominant. Blue: the counter part is IR log divergent and dominant. Red: the regularized spectrum is IR log divergent.

which just cancels all the UV divergences of the squared derivative $|(v_k/a)'|^2$ in (B.9). Similarly, the pressure is regularized by

$$p_k(\tau)_{reg} = \frac{k^5}{3\pi^2 a^4} \left| |v_k(\tau)|^2 - |v_k^{(4)}|^2 \right| \quad \text{for all } k, \quad (3.7)$$

where the adiabatic 4th order counter part in (A.16) is

$$\left| v_k^{(4)}(\tau) \right|^2 = \frac{1}{2k} + \frac{\beta(\beta+1)}{4k^3\tau^2} + \frac{3(\beta-1)\beta(\beta+1)(\beta+2)}{16k^5\tau^4}. \quad (3.8)$$

Fig.5 shows the resulting $\rho_k(\tau_1)_{reg}$, which is so drastically distorted that it becomes flat at lower frequencies $f < 10^9$ Hz. Moreover, at the IR end $k \sim 0$, it becomes IR logarithmic divergent. The situation with pressure is similar. This happens for all inflation models of $\beta \simeq -2$ other than $\beta = -2$. Recall that the original unregularized ρ_k and p_k in (2.36) (2.35) are IR convergent. Let us analyze the occurrence of IR divergence in details, with the pressure as example, by plotting each individual term schematically in Fig.6. The counter part (3.8) at small k gives

$$k^5 \left(\frac{1}{2k} + \frac{\beta(\beta+1)}{4k^3\tau_1^2} + \frac{3(\beta-1)\beta(\beta+1)(\beta+2)}{16k^5\tau_1^4} \right) \simeq \frac{3(\beta-1)\beta(\beta+1)(\beta+2)}{16\tau_1^4}, \quad (3.9)$$

which is a k -independent constant. Substituting (3.9) into the integration (2.30) will give a logarithmic divergent term

$$\frac{3(\beta-1)\beta(\beta+1)(\beta+2)}{16\tau_1^4} \int_0 \frac{dk}{k} = \infty,$$

so that p_{gw} becomes IR logarithmic divergent. Similar for the regularized energy density. This outcome at low k is a difficulty for the scheme of all- k regularization.

For de Sitter inflation, the scheme has another difficulty. The spectral energy density ρ_k in (2.32) has only one quartic divergent term, the counter terms $|(v_k^{(4)}/a)'|^2$ in (3.6) contain just one term $\frac{k}{2a^2}$, so that they cancel, yielding a zero energy. Similar for the spectral pressure p_k .

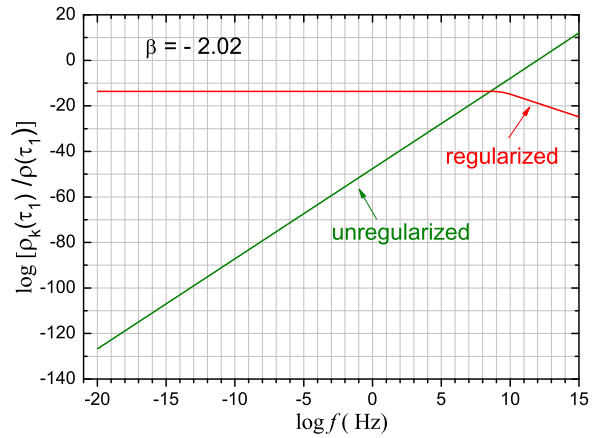


Figure 5: Red: the spectral energy density by the all- k regularization at τ_1 . Green: the unregularized. Rescaled by the background energy density $\rho(\tau_1)$ of inflation.

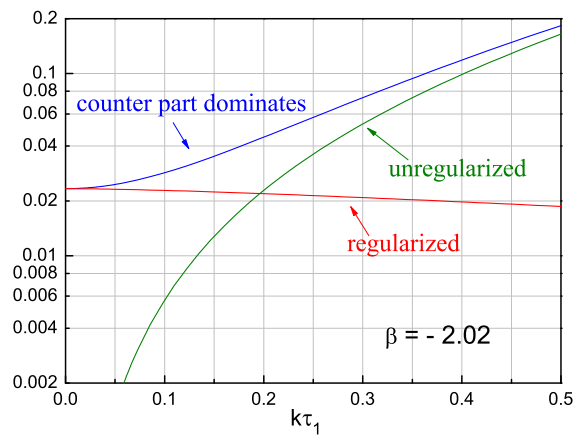


Figure 6: Schematically, Green: the unregularized pressure. Blue: the counter part dominates. Red: the regularized pressure.

4 Regularization inside the inflation horizon

We have seen in Fig.1 (a) that the unregularized power spectrum at a fixed time τ_1 rises up for $k \gtrsim 1/|\tau_1|$, and the UV divergences come from this high k range, whereas the low k range is irrelevant to UV divergence. This observation suggests that, to remove UV divergences, we need only regularize the k -modes whose wavelengths are inside the inflation horizon ($k \gtrsim 1/|\tau_1|$), and hold intact the k -modes outside the horizon.

For the power spectrum we propose the following scheme of regularization

$$\Delta_t^2(k, \tau)_{reg} = \frac{A^2 k^3}{\pi^2 a^2(\tau)} \begin{cases} (|v_k|^2 - |v_k^{(2)}|^2), & \text{for } k \geq \frac{1}{|\tau_1|}, \\ |v_k|^2, & \text{for } k < \frac{1}{|\tau_1|}. \end{cases} \quad (4.1)$$

The regularization is performed instantaneously at fixed τ_1 . We refer to this scheme also as the inflation-horizon regularization. This can apply at any time τ_1 during inflation, the spectrum regularized at an earlier time will evolve into the spectrum regularized at a later time. All the resulting spectra regularized at any instance during inflation are equivalent, in regard to post-inflation cosmology. Once the initial spectrum is made UV convergent, it will continue to be so in subsequent later stages. The power spectrum regularized at $\tau = 1000\tau_1$ and at τ_1 is shown in Fig.7 for $\beta = -2.02$, and in Fig.8 for $\beta = -1.98$, respectively. As expected, the low k portion is intact, whereas the UV divergences are gone, yielding a spectrum $\propto k^{-2}$ at high frequency end. For de Sitter inflation, the regularized power spectrum is nonvanishing in the whole range $f < 10^9\text{Hz}$ and is zero for $f > 10^9\text{Hz}$, as seen in Fig.9 (c). So the difficulty of the all k regularization is overcome.

By the way, for the scalar curvature perturbation [61–64] during inflation, the power spectrum has a similar structure to that of RGW [28], and can be also regularized by the inside-horizon regularization

$$\Delta_R^2(k, \tau)_{reg} = \frac{\beta + 1}{16(\beta + 2)} \Delta_t^2(k, \tau)_{reg} \quad (4.2)$$

for $\beta \neq -2$ in the exponential inflation model of Eq.(2.9). We mention that the CMB spectra C_l^{XX} induced by $\Delta_R^2(k, \tau)_{reg}$ are the same as those by the unregularized spectrum $\Delta_R^2(k, \tau)$, since its low k portion is unchanged under the inside-horizon regularization.

For ρ and p , parallel to (4.1), we have the inside-horizon regularization to 4th adiabatic order as the following

$$\rho_k(\tau)_{reg} = \frac{k^3}{\pi^2 a^2(\tau)} \begin{cases} \left| \left| \left(\frac{v_k}{a} \right)' \right|^2 - \left| \left(\frac{v_k^{(4)}}{a} \right)' \right|^2 \right|, & \text{for } k \geq \frac{1}{|\tau_1|}, \\ \left| \left(\frac{v_k}{a} \right)' \right|^2, & \text{for } k < \frac{1}{|\tau_1|}, \end{cases} \quad (4.3)$$

$$p_k(\tau)_{reg} = \frac{k^5}{3\pi^2 a^4(\tau)} \begin{cases} \left| |v_k|^2 - |v_k^{(4)}|^2 \right|, & \text{for } k \geq \frac{1}{|\tau_1|}, \\ |v_k|^2, & \text{for } k < \frac{1}{|\tau_1|}. \end{cases} \quad (4.4)$$

The resulting regularized spectra are plotted in Fig.9 (a) and (b), respectively. For de Sitter inflation, ρ_{kreg} is non-vanishing for $f < 10^9\text{Hz}$ and is zero for $f > 10^9\text{Hz}$, as shown in Fig.9 (d). And p_{kreg} is similar. Thus, the inside-horizon scheme overcomes the difficulty of the all- k scheme for de Sitter inflation.

At the level of the linearized approximation of Einstein equation, RGW is a linear field, and its k -modes are independent each other, there is no energy exchange between different

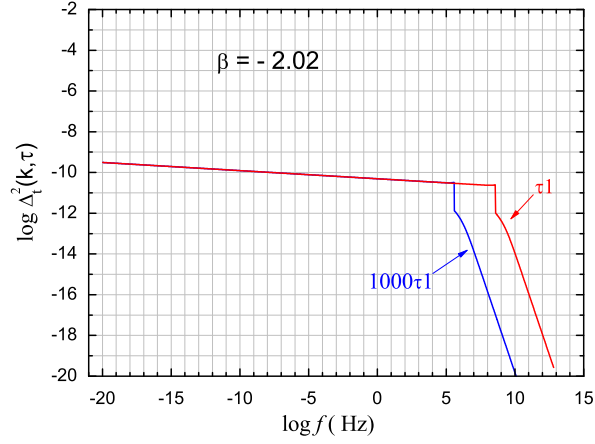


Figure 7: The spectrum regularized according to the inside-horizon regularization (4.1) at an earlier time $\tau = 1000\tau_1$, and at τ_1 , respectively. The former will evolve into the latter at τ_1 .

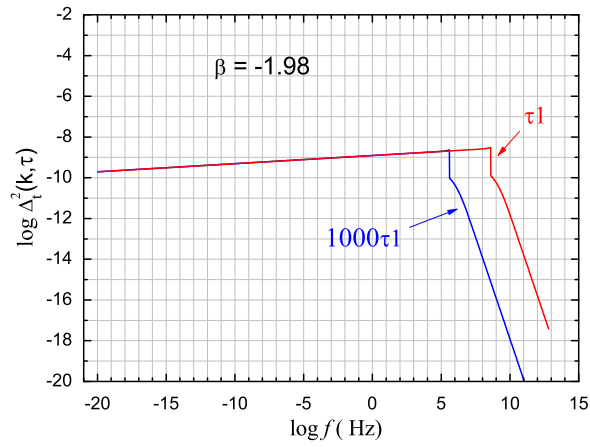


Figure 8: Similar to Fig.7, for the model $\beta = -1.98$.

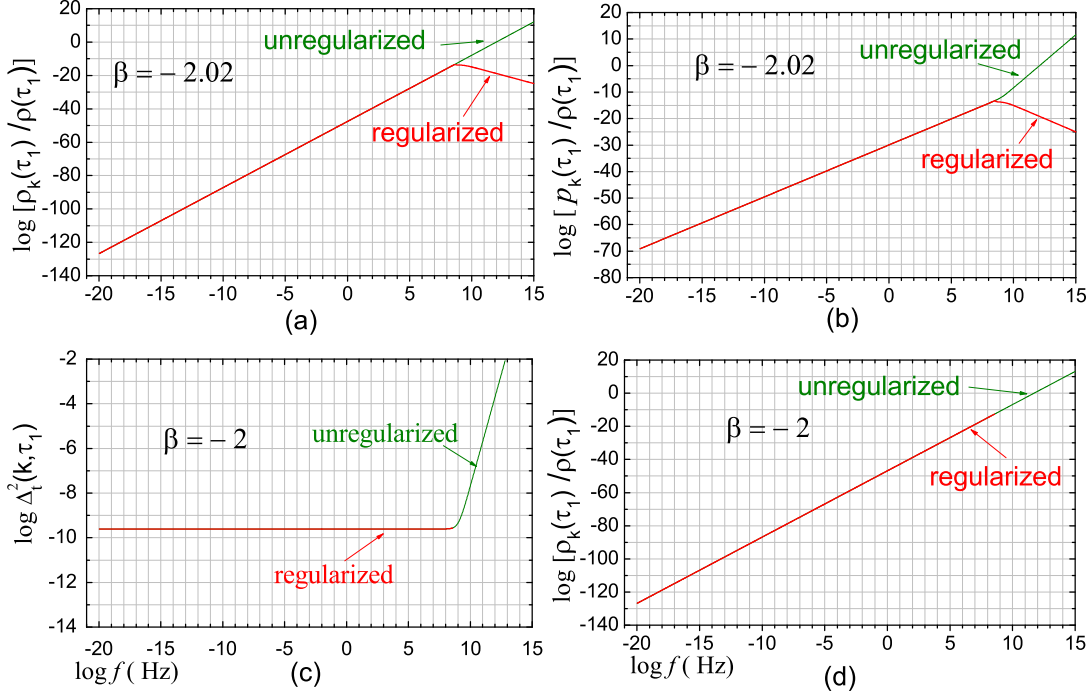


Figure 9: (a) $\rho_k(\tau_1)_{reg}$ by Eq.(4.3). (b) $p_k(\tau_1)_{reg}$ by Eq.(4.4). (c) $\Delta_t^2(k, \tau_1)_{reg} \neq 0$ for $f < 10^9$ Hz by (4.1) for de Sitter, (d) $\rho_k(\tau_1)_{reg} \neq 0$ for $f < 10^9$ Hz by Eq.(4.3) for de Sitter .

k -modes. Thus, the regularization inside the horizon will not affect the those outside the horizon. For the outside-horizon k -modes, $t_{\mu\nu}$ combined with other matter components is originally conserved [41, 42, 44, 45, 47]. The procedure of (4.3) (4.4) is equivalent to inserting a step function $\theta(k|\tau_1| - 1)$ in front of the subtraction term, where τ_1 is fixed, not a time variable. So time differentiation just passes over $\theta(k|\tau_1| - 1)$ which will not cause violation of conservation. Under the inside-horizon scheme the covariant conservation is respected by RGW together with other matter components. The scheme of inside-horizon regularization can be applied to other linear fields during inflation, such as free scalar fields, either massless or massive, as long as interaction between k -modes is vanishing, or negligibly small. This is the case also for the scalar curvature perturbation [28, 61] and the gauge-invariant perturbed scalar field [62–64], in the exponential inflation model of Eq.(2.9). As for the second order perturbation, there will be coupling between different k -modes of RGW, and between RGW and scalar metric perturbation [33, 34], this scheme may not apply directly.

The regularized energy density of RGW is finite, and satisfies the so-called back-reaction constraint. To be specific, at time τ_1 , we substitute $\rho_k(\tau_1)_{reg}$ into the integration (2.28) to get the regularized energy density

$$\rho_{gwareg} = \int_0^{k_1} \rho_k(\tau_1)_{reg} \frac{dk}{k} + \int_{k_1}^{\infty} \rho_k(\tau_1)_{reg} \frac{dk}{k}, \quad (4.5)$$

where $k_1 \equiv 1/|\tau_1|$. The first term of (4.5) is an integration over modes outside the horizon,

$\rho_k(\tau_1)$ can be approximated by $\frac{k^4}{2\pi^2 a^4(\tau_1)}$ of (2.32), so that

$$\int_0^{k_1} \rho_k(\tau_1)_{reg} \frac{dk}{k} \simeq \frac{H^4}{8\pi^2}. \quad (4.6)$$

In the second term of (4.5), $\rho_k(\tau_1)_{reg}$ has been given by (93) in Ref. [28], so that $\int_{k_1}^{\infty} \rho_k(\tau_1)_{reg} \frac{dk}{k} \sim \frac{(\beta+2)}{\pi^2} H^4 \ll H^4$. Hence, the sum is $\rho_{gw reg} \simeq \frac{H^4}{8\pi^2}$, which is much smaller than the background energy density $\frac{3}{8\pi G} H^2$.

5 Evolution of regularized spectra into the present

Taking the power spectrum by (4.1) as the initial condition, we let it evolve to the present stage. Inside the horizon $k|\tau_1| > 1$ the initial modes are taken to be

$$u_k^{reg}(\tau_1) = e^{i\theta(\tau_1)} \sqrt{|v_k(\tau_1)|^2 - |v_k^{(2)}(\tau_1)|^2}, \quad \text{for } k > \frac{1}{|\tau_1|} \quad (5.1)$$

with the phase $e^{i\theta(\tau_1)} = \frac{v_k(\tau_1)}{|v_k(\tau_1)|}$. Outside the horizon, the initial modes are the original $v_k(\tau_1)$. The subsequent evolution of each regularized mode is independent, and goes through reheating, radiation, matter, up to the present accelerating stage. Specifically, using the mode (5.1) and its time derivative of the inflation stage, we calculate the coefficients b_1, b_2 for the reheating stage, then for the subsequent stages (see Appendix C). This procedure results in a regularized mode $u_k(\tau_H)_{reg}$ at the present time τ_H , and the associated regularized power spectrum

$$\Delta_i^2(k, \tau_H)_{reg} = \frac{k^3}{\pi^2 a^2(\tau_H)} \frac{4}{M_{Pl}^2} |u_k(\tau_H)_{reg}|^2. \quad (5.2)$$

Here the mode $u_k(\tau_H)_{reg}$ of each k is actually a combination of positive and negative frequency k -modes. The spectrum is shown in Fig. 10 for $\beta = -2.02$, and in Fig.11 for $\beta = -2$ which is nonvanishing for $f < 10^9 \text{Hz}$. The detailed evolution history of regularized power spectrum in the course of cosmic expansion is demonstrated in Fig.12. The inside-horizon modes are decreasing as $h_k(\tau) \propto 1/a(\tau)$, and the outside-horizon modes keep constant $h_k(\tau) \propto \text{const}$, so that higher- k modes started decreasing earlier and has dropped more.

Now the evolution of ρ and p . The initial modes inside the horizon are taken to be

$$v_k^{reg}(\tau_1) = e^{i\theta(\tau_1)} \sqrt{|v_k(\tau_1)|^2 - |v_k^{(4)}(\tau_1)|^2}, \quad \text{for } k|\tau_1| > 1, \quad (5.3)$$

where $e^{i\theta(\tau_1)} = \frac{v_k(\tau_1)}{|v_k(\tau_1)|}$, and the outside-horizon initial modes are the original $v_k(\tau_1)$. The evolution results in the regularized modes $u_k(\tau_H)_{reg}$ at the present time, and the associated regularized spectral energy density and pressure

$$\rho_k(\tau_H)_{reg} = \frac{k^3}{\pi^2 a^2(\tau_H)} \left| \left(\frac{u_k(\tau_H)_{reg}}{a} \right)' \right|^2, \quad (5.4)$$

$$p_k(\tau_H)_{reg} = \frac{k^5}{3\pi^2 a^4(\tau_H)} |u_k(\tau_H)_{reg}|^2, \quad (5.5)$$

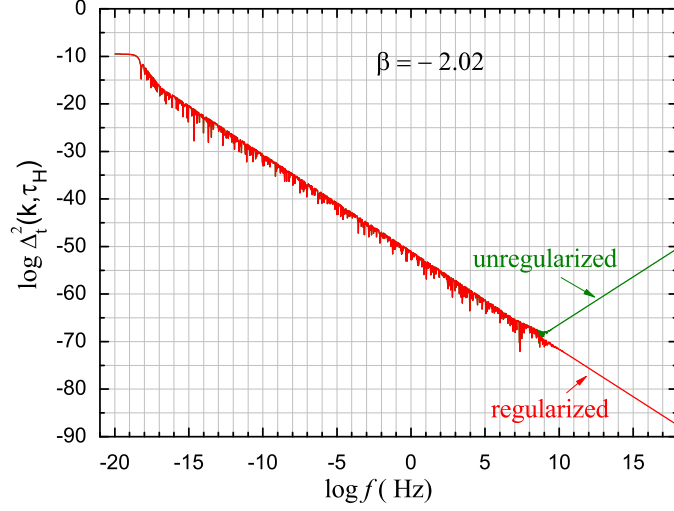


Figure 10: The present $\Delta_t^2(k, \tau_H)_{reg}$ which has evolved from the initial $\Delta_t^2(k, \tau_1)_{reg}$ in Fig.7. Its low frequency portion $f < 10^9$ Hz is overlapping with the unregularized.

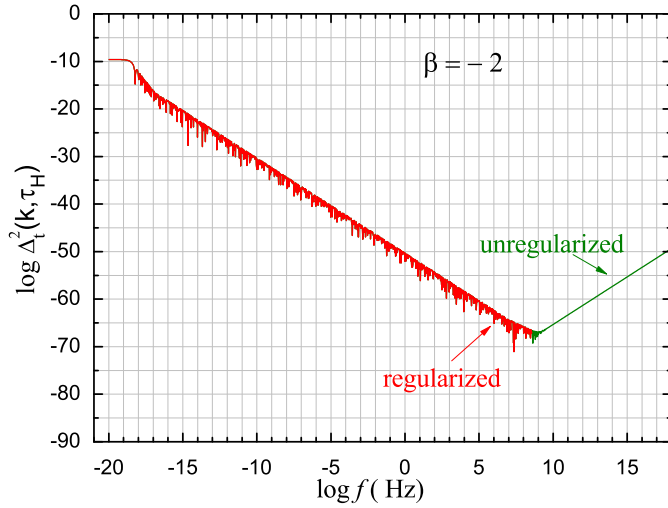


Figure 11: The present $\Delta_t^2(k, \tau_H)_{reg}$ is nonvanishing in the range $f < 10^9$ Hz, which has evolved from the initial $\Delta_t^2(k, \tau_1)_{reg}$ in Fig.9 (c).

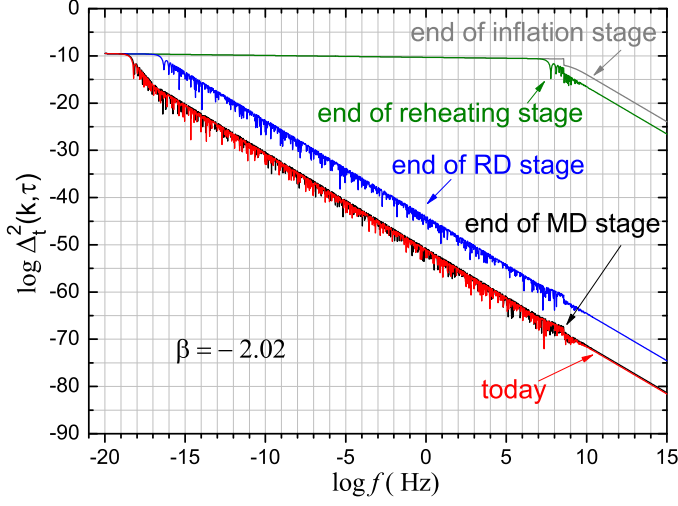


Figure 12: The evolution history of $\Delta_t^2(k, \tau)_{reg}$, from inflation, reheating, radiation, matter, up to the present accelerating stage.

$\rho_k(\tau_H)_{reg}$ is shown in Fig.13 (a) for $\beta = -2.02$ and Fig.13 (c) for $\beta = -2$, $p_k(\tau_H)_{reg}$ is shown in Fig.13 (b) for $\beta = -2.02$ and Fig.13 (d) for $\beta = -2$. They are rescaled by the critical density ρ_c in plotting. The detailed evolution history of the regularized spectral energy density is demonstrated in Fig.14.

We notice that the spectra after inflation all exhibit quick oscillations in frequency domain, whereas the initial spectra defined in BD vacuum during inflation have no oscillations. The oscillatory pattern is produced in the consecutive expansion stages, and is not changed by adiabatic regularization.

6 Structure of RGW and Interference

We analyze the structure of RGW as a quantum field in the present accelerating stage with the scale factor $a(\tau) = l_H |\tau - \tau_a|^{-\gamma}$ and $\gamma \simeq 2.1$. The solution (2.8) in the present stage is

$$u_k(\tau) = \sqrt{\frac{\pi}{2}} \sqrt{\frac{s}{2k}} \left[e^{-i\pi\gamma/2} \beta_k H_{-\gamma-\frac{1}{2}}^{(1)}(s) + e^{i\pi\gamma/2} \alpha_k H_{-\gamma-\frac{1}{2}}^{(2)}(s) \right], \quad \tau_E < \tau \leq \tau_H, \quad (6.1)$$

consisting of both positive and negative modes, where $s = k|\tau - \tau_a|$, the Bogolyubov coefficients β_k, α_k are determined by the cosmic evolution from initial condition. Their analytical expressions are obtained by connecting the modes u_k and u'_k for each k consecutively for the five stages. See Appendix C and Ref. [9, 10]. At high frequencies, they have the following asymptotic expressions:

$$\begin{aligned} \beta_k &= -\frac{i}{2z_E^2} e^{i(-x_1-t_1+t_s-y_s+y_2+z_2-z_E-s_E)+\frac{1}{2}i\pi\beta} \\ &+ i \left(\frac{1}{2z_E^2} - \frac{\gamma(\gamma+1)}{4s_E^2} \right) e^{i(-x_1-t_1+t_s-y_s+y_2-z_2+z_E-s_E)+\frac{1}{2}i\pi\beta} \end{aligned}$$

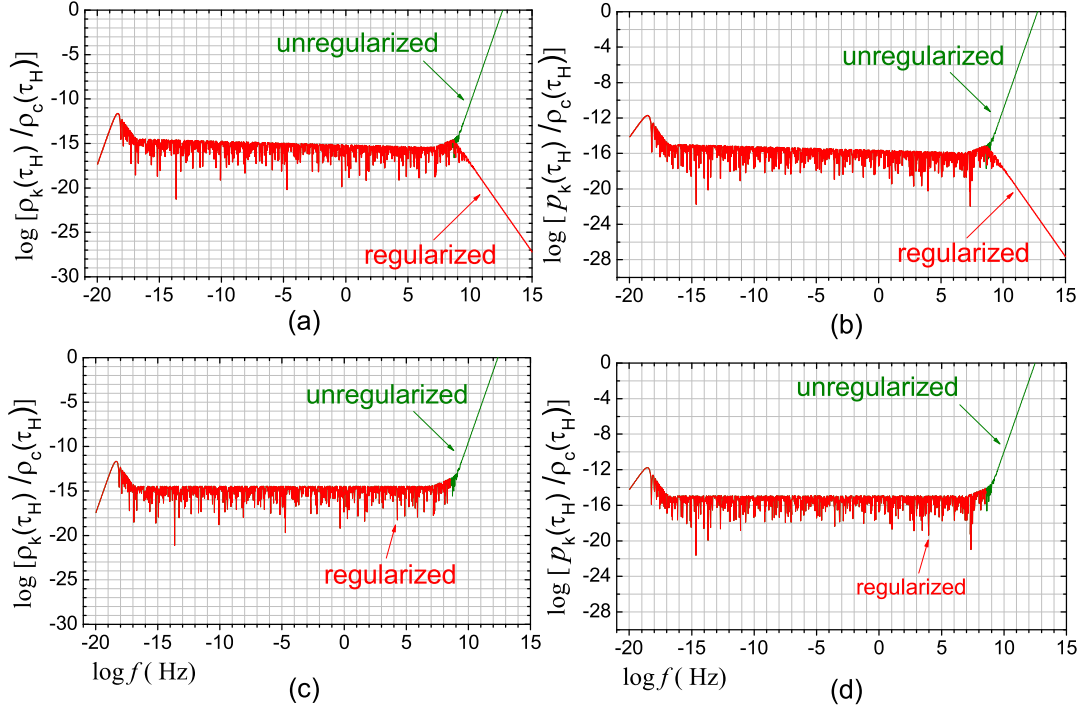


Figure 13: (a) $\Omega_g(\tau_H) = \rho_k(\tau_H)/\rho_c$ evolved from the initial $\rho_k(\tau_1)_{reg}$ in Fig.9 (a). (b) $p_k(\tau_H)/\rho_c$ evolved from $p_k(\tau_1)_{reg}$ in Fig.9 (b). (c) (d) For de Sitter inflation, $\Omega_g(\tau_H) \neq 0$, $p_k(\tau_H)/\rho_c \neq 0$ for $f < 10^9$ Hz.

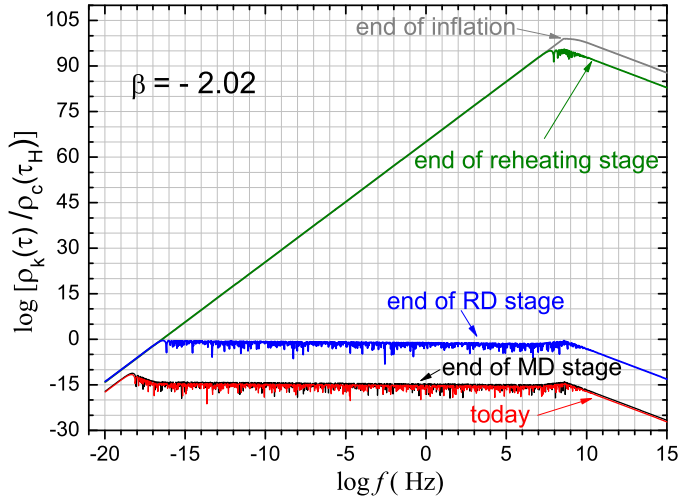


Figure 14: The evolution history of $\rho_k(\tau)_{reg}$ from the end of inflation up to the present.

$$\begin{aligned}
& +i \left(\frac{\beta(\beta+1)}{4x_1^2} - \frac{\beta_s(\beta_s+1)}{4t_1^2} \right) e^{i(-x_1+t_1-t_s+y_s-y_2+z_2-z_E-s_E)+\frac{1}{2}i\pi\beta} \\
& +i \frac{\beta_s(\beta_s+1)}{4t_s^2} e^{i(-x_1-t_1+t_s+y_s-y_2+z_2-z_E-s_E)+\frac{1}{2}i\pi\beta} + \mathcal{O}(k^{-3}), \tag{6.2}
\end{aligned}$$

$$\begin{aligned}
\alpha_k = & i \left(1 - i \frac{\beta(\beta+1)}{2x_1} - i \frac{\beta_s(\beta_s+1)}{2t_1} + i \frac{\beta_s(\beta_s+1)}{2t_s} - i \frac{1}{z_2} + i \frac{1}{z_E} + i \frac{\gamma(\gamma+1)}{2s_E} \right. \\
& - \frac{\beta^2(\beta+1)^2}{8x_1^2} - \frac{\beta_s^2(\beta_s+1)^2}{8t_1^2} - \frac{\beta_s^2(\beta_s+1)^2}{8t_s^2} - \frac{1}{2z_2^2} - \frac{1}{2z_E^2} - \frac{\gamma^2(\gamma+1)^2}{8s_E^2} \\
& - \frac{\beta(\beta+1)\beta_s(\beta_s+1)}{4x_1t_1} + \frac{\beta(\beta+1)\beta_s(\beta_s+1)}{4x_1t_s} - \frac{\beta(\beta+1)}{2x_1z_2} + \frac{\beta(\beta+1)}{2x_1z_E} \\
& + \frac{\beta(\beta+1)\gamma(\gamma+1)}{4x_1s_E} + \frac{\beta_s^2(\beta_s+1)^2}{4t_1t_s} - \frac{\beta_s(\beta_s+1)}{2t_1z_2} + \frac{\beta_s(\beta_s+1)}{2t_1z_E} \\
& + \frac{\beta_s(\beta_s+1)\gamma(\gamma+1)}{4t_1s_E} + \frac{\beta_s(\beta_s+1)}{2t_sz_2} - \frac{\beta_s(\beta_s+1)}{2t_sz_E} \\
& - \frac{\beta_s(\beta_s+1)\gamma(\gamma+1)}{4t_s s_E} + \frac{1}{z_2z_E} + \frac{\gamma(\gamma+1)}{2z_2s_E} \\
& \left. - \frac{\gamma(\gamma+1)}{2z_E s_E} \right) e^{i(-x_1-t_1+t_s-y_s+y_2-z_2+z_E+s_E)+\frac{1}{2}i\pi\beta} + \mathcal{O}(k^{-3}), \tag{6.3}
\end{aligned}$$

where $x_1, t_1, t_s, y_s, y_2, \dots, s_E$ are the time instances of transitions multiplied by k . See Appendix C. (In (43) and (44) of Ref. [28] x_1 and s_E should have minus signs.) We plot $|\alpha_k|^2$ and $|\beta_k|^2$ as functions of k in Fig.15. They satisfy the relation

$$|\alpha_k|^2 - |\beta_k|^2 = 1, \tag{6.4}$$

which is implied by applying the Wronskian (2.11). The relation (6.4) can be checked to be satisfied by (6.2) and (6.3) to each order of powers of k . The positive frequency mode in (6.1) is taken as the vacuum mode at the present stage

$$v_k(\tau) = \sqrt{\frac{\pi}{2}} \sqrt{\frac{s}{2k}} e^{i\pi\gamma/2} H_{-\gamma-\frac{1}{2}}^{(2)}(s), \tag{6.5}$$

such that $v_k(\tau) \rightarrow \frac{1}{\sqrt{2k}} e^{-ik(\tau-\tau_a)}$ as $k \rightarrow \infty$. Then the mode solution (6.1) is written as

$$u_k(\tau) = \alpha_k v_k(\tau) + \beta_k v_k^*(\tau). \tag{6.6}$$

Starting from the vacuum fluctuation during inflation with only positive-frequency modes (2.13), RGW has evolved into a mixture of the positive and negative frequency modes as in Eq.(6.6). The field operator h_{ij} in Eq.(2.2) in the present stage, for each \mathbf{k} and each s polarization, is proportional to

$$\begin{aligned}
& \left[a_{\mathbf{k}}^s h_{\mathbf{k}}^s(\tau) e^{i\mathbf{k}\cdot\mathbf{x}} + a_{\mathbf{k}}^{s\dagger} h_{\mathbf{k}}^{s*}(\tau) e^{-i\mathbf{k}\cdot\mathbf{x}} \right] \\
& = \frac{A}{a(\tau)} \left[a_{\mathbf{k}} \alpha_k v_k e^{i\mathbf{k}\cdot\mathbf{x}} + a_{\mathbf{k}}^\dagger \beta_k^* v_k e^{-i\mathbf{k}\cdot\mathbf{x}} + a_{\mathbf{k}} \beta_k v_k^* e^{i\mathbf{k}\cdot\mathbf{x}} + a_{\mathbf{k}}^\dagger \alpha_k^* v_k^* e^{-i\mathbf{k}\cdot\mathbf{x}} \right] \\
& = \frac{A}{a(\tau)} \left[A_{\mathbf{k}} v_k e^{i\mathbf{k}\cdot\mathbf{x}} + A_{\mathbf{k}}^\dagger v_k^* e^{-i\mathbf{k}\cdot\mathbf{x}} \right].
\end{aligned}$$

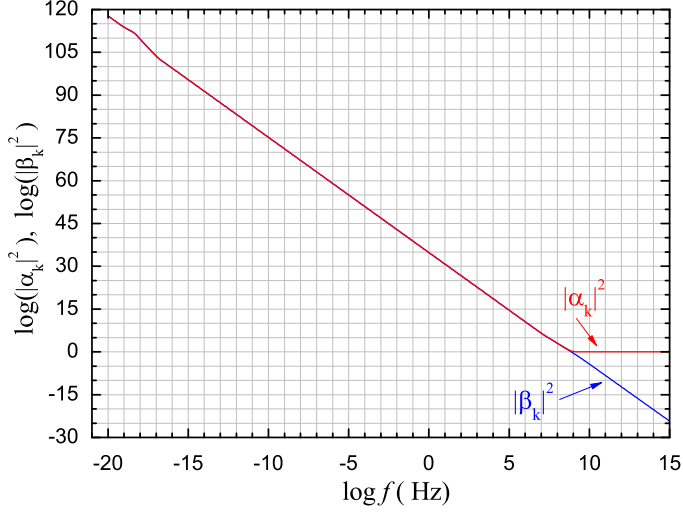


Figure 15: Blue: $|\alpha_k|^2$. Red: $|\beta_k|^2$. The relation $|\alpha_k|^2 - |\beta_k|^2 = 1$ holds.

The above terms will appear in the summation over \mathbf{k} , so one can change the sign of the wavevector \mathbf{k} in the β_k terms. Thus

$$h_{ij}(\mathbf{x}, \tau) = \int \frac{d^3k}{(2\pi)^{3/2}} \sum_{s=+, \times} \hat{\epsilon}_{ij}(k) \frac{A}{a(\tau)} \left[A_{\mathbf{k}} v_k(\tau) e^{i\mathbf{k}\cdot\mathbf{x}} + A_{\mathbf{k}}^\dagger v_k^*(\tau) e^{-i\mathbf{k}\cdot\mathbf{x}} \right], \quad (6.7)$$

where

$$A_{\mathbf{k}} \equiv \alpha_k a_{\mathbf{k}} + \beta_k^* a_{-\mathbf{k}}^\dagger \quad (6.8)$$

is interpreted as the annihilation operator of gravitons of \mathbf{k} for the present stage. (In the expression of $A_{\mathbf{k}}$ in Ref. [28] where the subscript should have a minus sign, $a_{\mathbf{k}}^\dagger \rightarrow a_{-\mathbf{k}}^\dagger$.) The number density of gravitons in k -mode in the present stage is

$$N_{\mathbf{k}} = \langle 0 | A_{\mathbf{k}}^\dagger A_{\mathbf{k}} | 0 \rangle = |\beta_k|^2, \quad (6.9)$$

which has been generated during the expansion.

By Eqs.(6.4) (6.6), we write the power spectrum (2.19), the spectral energy density (2.29) and pressure (2.31) at the present time

$$\Delta_t^2(k, \tau_H) = \frac{A^2 k^3}{\pi^2 a^2} (|v_k|^2 + 2\text{Re}(\alpha_k \beta_k^* v_k^2) + 2|\beta_k|^2 |v_k|^2), \quad (6.10)$$

$$\rho_k(\tau_H) = \frac{k^3}{\pi^2 a^2} \left(\left| \left(\frac{v_k}{a} \right)' \right|^2 + 2\text{Re}[\alpha_k \beta_k^* \left(\frac{v_k}{a} \right)'^2] + 2|\beta_k|^2 \left| \left(\frac{v_k}{a} \right)' \right|^2 \right), \quad (6.11)$$

$$p_k(\tau_H) = \frac{k^5}{3\pi^2 a^4} (|v_k|^2 + 2\text{Re}(\alpha_k \beta_k^* v_k^2) + 2|\beta_k|^2 |v_k|^2), \quad (6.12)$$

all of them contain three terms. Consider Eq.(6.10) as example, the first term $|v_k|^2$ is the present vacuum contribution. $2|\beta_k|^2 |v_k|^2$ is the graviton contribution. $2\text{Re}(\alpha_k \beta_k^* v_k^2)$ is the interference between the positive and negative frequency modes. (It was also called

as the vacuum-graviton coupling in Paper I.) These interpretations also apply to (6.11) and (6.12). The interference arises inevitably as soon as the negative frequency modes $\beta_k v_k^*$ are developed in the reheating stage after inflation and in the subsequent stages. Hence, the particle production in the expanding RW spacetime is always accompanied by the interference. In this sense, the interference is a prediction of quantum field theory in curved spacetime.

The contributions of the three terms vary in different frequency ranges and are plotted in Fig.16 for the unregularized power spectrum. Over the range $f \leq 10^9 \text{Hz}$, the graviton term is dominant, the oscillatory interference term is comparable, and the vacuum term is negligibly small. For $f \geq 10^9 \text{Hz}$, the vacuum dominates and is $\propto k^2$ quadratic divergent, the interference is $\propto k^0$ logarithmic divergent, the graviton is $\propto k^{-2}$ UV convergent.

Fig.17 is an enlarged portion of Fig.16 for $f \lesssim 10^{-17} \text{Hz}$. This portion corresponds to the range probed by CMB anisotropies [28, 30, 31].

Fig.18 (a) shows the range around $f \sim 10^{-9} \text{Hz}$ corresponding to that of PTA detectors. In this range the characteristic amplitude $h(f, \tau_H) \equiv \sqrt{\Delta_t^2(k, \tau_H)} \sim 10^{-17}$ is high and may be possibly detected by PTA detectors, such as PPTA, EPTA, SKA, NANOGrav, FAST, etc [52–57]. The oscillation frequency of interference is $\sim 8 \times f \sim 10^{-8} \text{Hz}$ and the oscillatory amplitude is $\sim 10^{-33}$ decreasing at large f . This unique oscillatory feature existing will be helpful to distinguish the RGW signal from the GW foreground.

Fig.18 (b) shows the range around $f \sim 10^{-2} \text{Hz}$ corresponding to LISA [58, 59]. The characteristic amplitude $h(f, \tau_H) \sim 10^{-23}$, the oscillation frequency $\sim 10 \times f \sim 10^{-1} \text{Hz}$.

Fig.18 (c) shows the range around $f \sim 10^2 \text{Hz}$ corresponding to LIGO [60], the oscillation frequency $\sim 18 \times f \sim 10^3 \text{Hz}$.

Fig.18 (d) shows the high frequency portion around $f \sim 10^9 \text{Hz}$. This may be explored high-frequency Gaussian beam detectors [11, 12].

From Figs.18 (a),(b),(c) one sees that the oscillation amplitude of interference is comparable to that of the vacuum, the latter actually forms the upper envelope of the oscillatory interference. The oscillation amplitude decreases with and the oscillation frequency increases with the spectrum frequency f . However, the details of interference depend on the regularization scheme, and its extent may be changed in other schemes. Future detections of RGW will have chance to probe these.

7 Regularization at the present time

As possible alternative to that in Section 5, we try to perform regularization at the present time. The three terms in the power spectrum (6.10) need to be regularized. As before, the vacuum term is subtracted by $|v_k^{(2)}|^2$ which is the 2nd adiabatic order counter term for the present stage (see (A.13) in Appendix A). The interference term $Re(\alpha_k \beta_k^* v_k^2)$ is subtracted by $(v_k^{(0)})^2$, which is the 0th order counter term given in (A.14). The graviton term $|\beta_k|^2 |v_k|^2 \propto k^{-5}$ is already UV convergent and needs no regularization. So the power spectrum is regularized at the present time as the following

$$\begin{aligned} \Delta_t^2(k, \tau_H)_{reg} = & \frac{A^2 k^3}{\pi^2 a^2(\tau_H)} \left[\left(|v_k|^2 - \left(\frac{1}{2k} + \frac{\gamma(\gamma+1)}{4k^3(\tau_H - \tau_a)^2} \right) \right) \right. \\ & \left. + 2Re \left(\alpha_k \beta_k^* \left(v_k^2 - \frac{e^{-2ik(\tau_H - \tau_a)}}{2k} \right) \right) + 2|\beta_k|^2 |v_k|^2 \right]. \end{aligned} \quad (7.1)$$

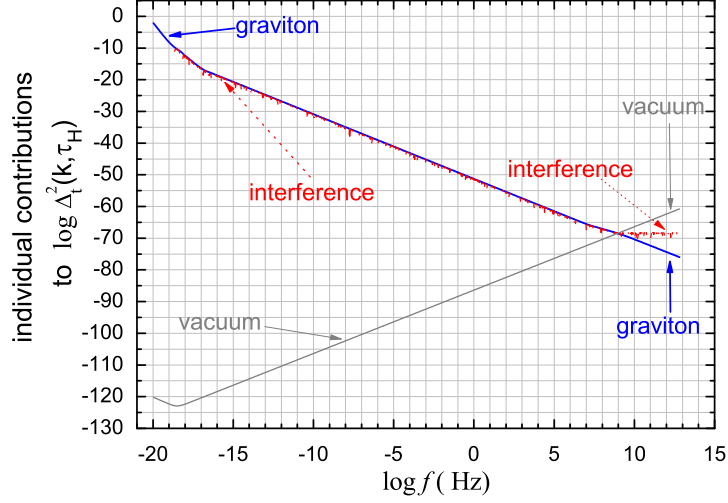


Figure 16: The individual contributions to unregularized power spectrum by the vacuum, interference, and graviton. The interference has negative values which are not shown in log plot.

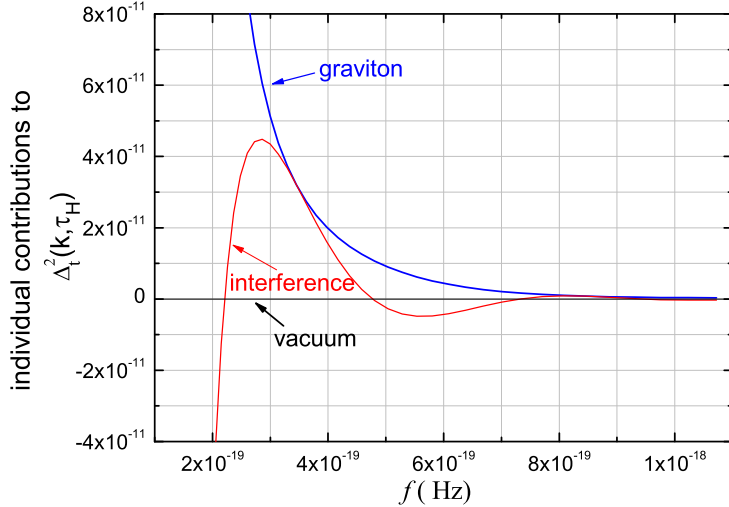


Figure 17: The enlarged portion of Fig. 16 at low frequency end $f \lesssim 10^{-17}\text{Hz}$, corresponding to large angular CMB anisotropies and polarization. The graviton dominates, the interference is oscillatory, the vacuum is negligibly small.

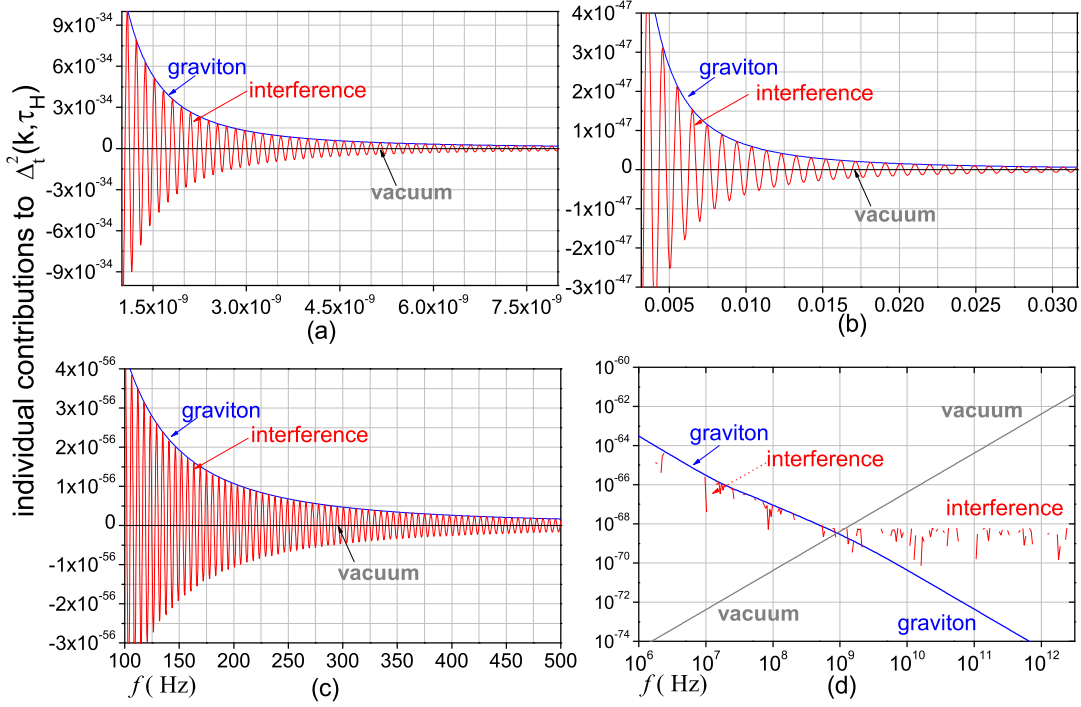


Figure 18: (a): Around $f \sim 10^{-9}$ Hz, for PTA. (b): Around $f \sim 10^{-2}$ Hz, for LISA. (c): Around $f \sim 10^2$ Hz, for LIGO. (d): Around $f \sim 10^9$ Hz, for Gauss-beam detector.

The spectral energy density (6.11) and pressure (6.12) are regularized up to the 4th adiabatic order

$$\begin{aligned} \rho_k(\tau_H)_{reg} = & \frac{k^3}{\pi^2 a^2} \left| \left| \left(\frac{v_k}{a} \right)' \right|^2 - \left| \left(\frac{v_k^{(4)}}{a} \right)' \right|^2 + 2\text{Re} \left[\alpha_k \beta_k^* \left(\left(\frac{v_k}{a} \right)' \right)^2 - \left(\frac{v_k^{(2)}}{a} \right)' \right]^2 \right. \\ & \left. + 2|\beta_k|^2 \left(\left| \left(\frac{v_k}{a} \right)' \right|^2 - \left| \left(\frac{v_k^{(0)}}{a} \right)' \right|^2 \right) \right|, \end{aligned} \quad (7.2)$$

$$\begin{aligned} p_k(\tau_H)_{re} = & \frac{k^5}{3\pi^2 a^4} \left| |v_k|^2 - |v_k^{(4)}|^2 + 2\text{Re} \left[\alpha_k \beta_k^* (v_k^2 - (v_k^{(2)})^2) \right] \right. \\ & \left. + 2|\beta_k|^2 (|v_k|^2 - |v_k^{(0)}|^2) \right|, \end{aligned} \quad (7.3)$$

where six counter terms are listed in (A.7)–(A.12) in Appendix A, giving the explicit formulae

$$\begin{aligned} \rho_k(\tau_H)_{reg} = & \frac{k^3}{\pi^2 a^2} \left| \left| \left(\frac{v_k}{a} \right)' \right|^2 - \frac{k}{a^2} \left(\frac{1}{2} + \frac{\gamma(\gamma-1)}{4k^2\tau^2} + \frac{3(\gamma-2)(\gamma-1)\gamma(\gamma+1)}{16k^4\tau^4} \right) \right. \\ & \left. + 2\text{Re} \left(\alpha_k \beta_k^* \left[\left(\frac{v_k}{a} \right)' \right]^2 - \frac{ke^{-2ik\tau}}{2a^2} \left(-1 + i \frac{\gamma(\gamma-1)}{k\tau} \right. \right. \right. \right. \\ & \left. \left. \left. + \frac{\gamma(\gamma-1)(\gamma^2-\gamma-1)}{2k^2\tau^2} \right) \right] \right) + 2|\beta_k|^2 \left| \left| \left(\frac{v_k}{a} \right)' \right|^2 - \frac{k}{2a^2} \right|, \end{aligned} \quad (7.4)$$

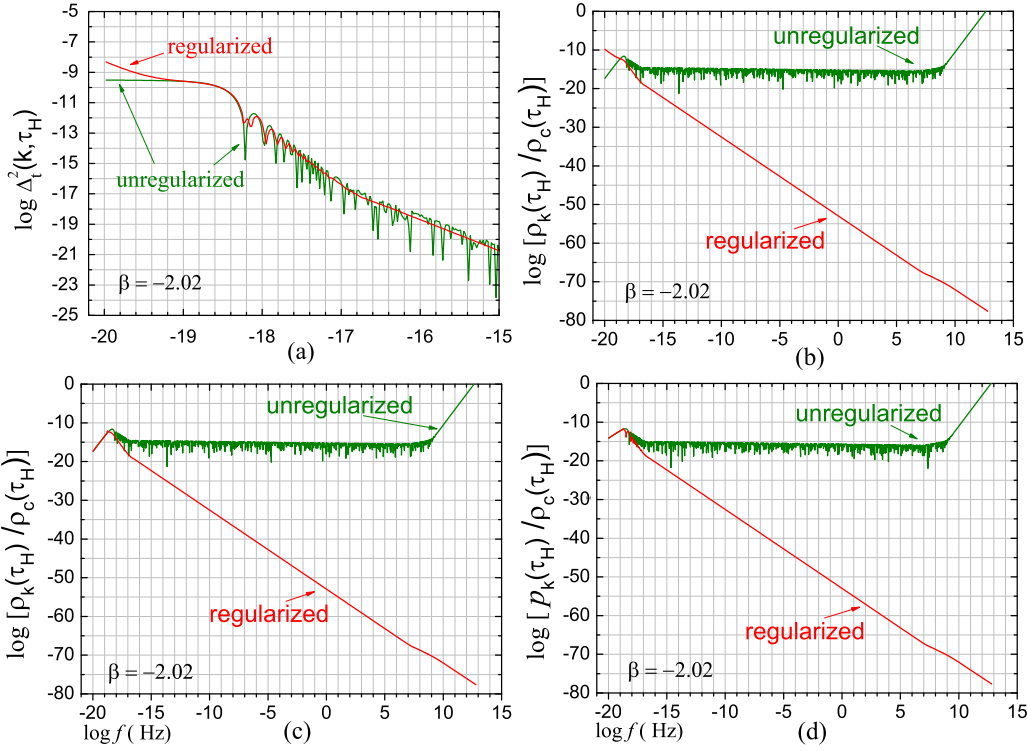


Figure 19: (a) Δ_l^2 regularized at τ_H for all k has distortions at low frequency end. (b) ρ_k regularized at τ_H for all k is drastically distorted. (c) (d) ρ_k and p_k regularized at τ_H for $k > \frac{1}{|\tau_H - \tau_a|}$ are also drastically distorted.

$$\begin{aligned}
p_k(\tau_H)_{re} &= \frac{k^5}{3\pi^2 a^4} \left| |v_k|^2 - \frac{1}{2k} \left(1 + \frac{\gamma(\gamma+1)}{2k^2 \tau^2} + \frac{3(\gamma+2)(\gamma+1)\gamma(\gamma-1)}{8k^4 \tau^4} \right) \right. \\
&\quad \left. + 2Re \left(\alpha_k \beta_k^* \left[v_k^2 - \frac{e^{-2ik\tau}}{2k} \left(1 - i \frac{\gamma(\gamma+1)}{k\tau} - \frac{\gamma(\gamma+1)(\gamma^2 + \gamma - 1)}{2k^2 \tau^2} \right) \right] \right) \right. \\
&\quad \left. + 2|\beta_k|^2 \left(|v_k|^2 - \frac{1}{2k} \right) \right|. \tag{7.5}
\end{aligned}$$

In the above, τ stands for $(\tau_H - \tau_a)$ to avoid clumsy notation.

If the formulae (7.1) (7.4) (7.5) are applied for all k -modes, the resulting power spectrum shown in Fig.19 (a) is uplifted at $k \sim 0$, the interference oscillations are suppressed. The resulting $\rho_k(\tau_H)_{reg}$ is totally distorted as shown in Fig.19 (b). The pressure has a similar situation. Thus, the all- k regularization at the present time is unsuccessful.

If (7.1)(7.4) (7.5) are applied to the modes inside the present horizon $k > \frac{1}{|\tau_H - \tau_a|}$, corresponding to $f > \frac{H_0}{2\pi} \sim 10^{-19}$ Hz. Again, $\rho_k(\tau_H)_{reg}$ is drastically distorted, as shown in Fig.19 (c). This scheme is unsuccessful either.

An inspection tells that all three unregularized spectra rise up at $f \gtrsim 10^9$ Hz which corresponds to $k > 1/|\tau_1|$ by the relation (2.25). So, the present k -modes that carry UV divergences are identified as the same modes that were carrying UV divergences during inflation. Therefore, we try to apply the formulae (7.1) (7.4) (7.5) only to the high k -modes with $f > 10^9$ Hz, and hold the low k intact. The resulting power spectrum shown in Fig.20 (a) has no distortion for $f < 10^9$ Hz, similar to Fig.10. However, at high frequency as shown in Fig.20 (b), it behaves as $\propto k^{-2}$ in the range $(10^9 \sim 10^{35})$ Hz, and as $\propto k^{-1}$

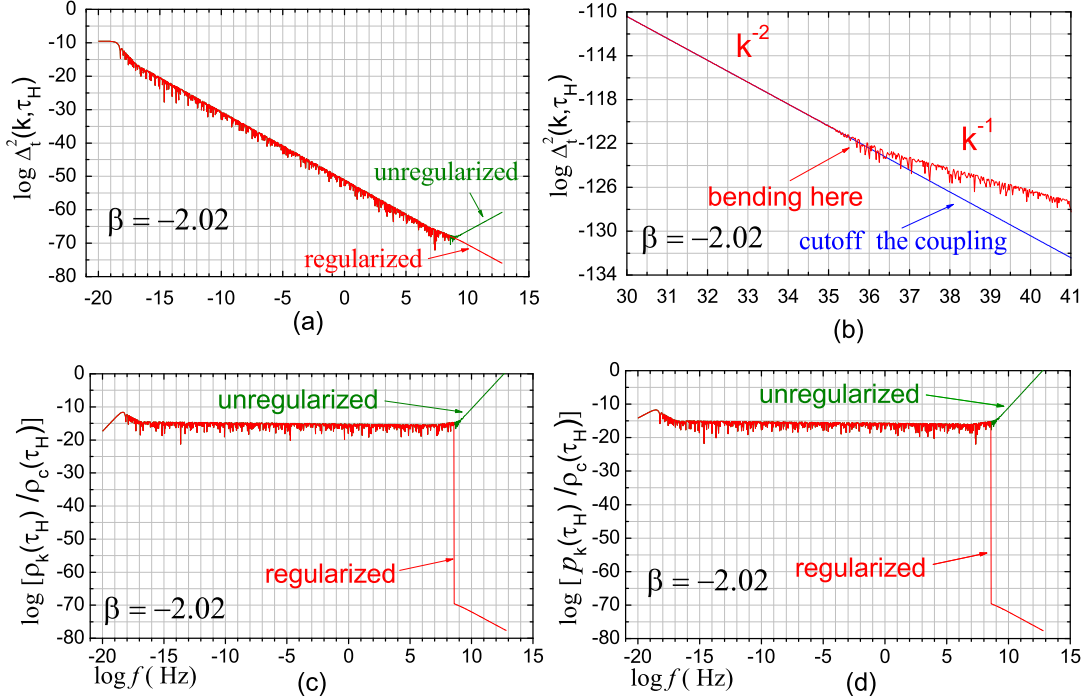


Figure 20: (a) $\Delta_t^2(k, \tau_H)_{reg}$ regularized at τ_H for $f > 10^9$ Hz. (b) The high frequency end of (a) has a bending at $f \sim 10^{35}$ Hz. (c) (d) $\rho_k(\tau_H)_{reg}$ and $p_k(\tau_H)_{reg}$ regularized at τ_H for $f > 10^9$ Hz.

for $f > 10^{35}$ Hz, giving rise to a bending. This differs from an unbending result $\propto k^{-2}$ in Paper I where a cutoff was made on the interference term. The spectral energy density and pressure shown in Fig.20 (c) (d) have no distortion for $f < 10^9$ Hz, similar to Fig.13, but have an abrupt drop at $f \simeq 10^9$ Hz. Thus, this scheme yields the high-frequency irregularities, which seem artificial. The actual spectra at high frequency may eventually be explored by high-frequency Gaussian beam detectors [11, 12].

8 Conclusion and Discussion

The power spectrum of RGW contains UV divergences up to 2nd adiabatic order, and the energy density and pressure of RGW contain UV divergences up to 4th order, the scheme of all- k regularization removes UV divergences, but also brings about distortions at low frequencies. More severely, as our analysis has revealed, the spectral energy density and pressure are even changed to IR divergent under the all- k regularization.

To avoid these low-frequency distortions, we have proposed the scheme of inside-horizon regularization at a fixed instance during inflation. This is motivated by the fact that the UV divergences are due to the short-wavelength modes inside the horizon, whereas the long-wavelength modes are not responsible. We regularize only the inside-horizon modes and keep the outside-horizon modes intact. Consequently, the regularized spectra all become UV convergent, and simultaneously are free of IR distortions for a whole range of $f \lesssim 10^9$ Hz, as shown in Figs.7, 8, 9. With these spectra as the initial condition, we let them evolve, and obtain the present spectra in Fig.10 and Fig.13, which all remain UV convergent and free of IR distortion. For de Sitter inflation, the scheme

yields the spectra, which are non-vanishing and free of IR distortion, as shown in Fig.11 and Fig.13, thus, overcoming the difficulty with the all- k regularization that would inevitably lead to vanishing spectra. It is legitimate to adopt the inside-horizon scheme of regularization for RGW, because at the level of the linearized Einstein equation, k -modes of RGW are linearly independent. The inside-horizon scheme can apply also to other linear fields such as the scalar curvature perturbation and the gauge-invariant perturbed scalar field during inflation.

Three schemes of regularization at the present time have been explored and are found to give some irregularities. Thus, the inside-horizon scheme at the end of inflation is preferable to these three, since it yields the UV-convergent spectra from start which are free of low-frequency distortion. Nevertheless, even our inside-horizon scheme presented in this paper may be not the final prescription, other possible valid schemes can also exist, because generally there is no unique adiabatic regularization from the perspective of renormalization.

We have also analyzed the structure of spectra of RGW as quantum field at the present stage, consisting of the graviton, the interference, and the vacuum contributions. The former two contributions are dominant in the range $f \lesssim 10^9\text{Hz}$, which covers almost all the observational band of detectors. As a prominent feature, the spectra contain quick oscillations in the frequency domain, as plotted in Figs.17 and 18. This oscillatory pattern is due to interference of positive and negative frequency modes of RGW. Since the interference depends on the regularization schemes, and no final conclusive scheme has been arrived so far, we shall leave this to be probed by future RGW detections.

Acknowledgements

Y. Zhang is supported by NSFC Grant No. 11421303, 11675165, 11633001 SRFDP, and CAS, the Strategic Priority Research Program “The Emergence of Cosmological Structures” of the Chinese Academy of Sciences, Grant No. XDB09000000.

Appendix

A The adiabatic counter terms up to 4th order

In this appendix, we calculate the adiabatic counter terms and list explicitly their analytical expressions that have been used in the context. See also Refs. [13, 15, 65] for a scalar field. For RGW in a RW spacetime, the n -th adiabatic mode for an integer $n \geq 0$ is

$$v_k^{(n)}(\tau) = \frac{1}{\sqrt{2W_k^{(n)}(\tau)}} \exp \left[-i \int_{\tau_0}^{\tau} W_k^{(n)}(\tau') d\tau' \right], \quad (\text{A.1})$$

where

$$W_k^{(n)} = \sqrt{k^2 - \frac{a''}{a} - \frac{1}{2} \left[\frac{W_k^{(n-2)''}}{W_k^{(n-2)}} - \frac{3}{2} \left(\frac{W_k^{(n-2)'}}{W_k^{(n-2)}} \right)^2 \right]}. \quad (\text{A.2})$$

To the 0th order, $W_k^{(0)} = k$, $v_k^{(0)} = \frac{1}{\sqrt{2k}}e^{-ik\tau}$, which corresponds to the mode in Minkowski spacetime. To the 2th adiabatic order $W_k^{(2)} = \sqrt{k^2 - \frac{a''}{a}}$, the 4th adiabatic order

$$W_k^{(4)} = k\sqrt{1 - \frac{a''}{k^2 a} - \frac{1}{4k^4 a^2}(a''^2 - aa'''' + 2a'a''' - 2\frac{a'^2 a''}{a})}. \quad (\text{A.3})$$

By the construction, the 4th order adiabatic mode $v_k^{(4)}$ satisfies the wave equation (2.7) to 4th order, and respects the covariant conservation to 4th order. Similar for the 2nd order adiabatic mode $v_k^{(2)}$.

For the accelerating stage $a(\tau) \propto |\tau|^{-\gamma}$,

$$\begin{aligned} W_k^{(4)} &= k\sqrt{1 - \frac{\gamma(\gamma+1)}{k^2 \tau^2} + \frac{6\gamma(\gamma+1)}{4k^4 \tau^4}} \\ &\simeq k\left(1 - \frac{\gamma(\gamma+1)}{2k^2 \tau^2} - \frac{\gamma(\gamma-2)(\gamma+1)(\gamma+3)}{8k^4 \tau^4}\right). \end{aligned} \quad (\text{A.4})$$

Substituting this into (A.1) yields the 4th adiabatic mode

$$\begin{aligned} v_k^{(4)}(\tau) &\simeq \frac{e^{-ik\tau}}{\sqrt{2k}}\left(1 - i\frac{\gamma(\gamma+1)}{2k\tau} - \frac{(\gamma+2)(\gamma+1)\gamma(\gamma-1)}{8k^2 \tau^2}\right. \\ &\quad \left.+ i\frac{(\gamma-2)(\gamma-1)\gamma(\gamma+1)(\gamma+2)(\gamma+3)}{48k^3 \tau^3}\right), \end{aligned} \quad (\text{A.5})$$

and the 2nd order adiabatic counter mode follows

$$v_k^{(2)}(\tau) = \frac{e^{-ik\tau}}{\sqrt{2k}}\left(1 - i\frac{\gamma(\gamma+1)}{2k\tau} - \frac{(\gamma+2)(\gamma+1)\gamma(\gamma-1)}{8k^2 \tau^2}\right). \quad (\text{A.6})$$

From these counter modes, one obtains the adiabatic counter terms that are used in the context. The time derivatives are

$$\left|\left(\frac{v_k^{(4)}(\tau)}{a}\right)'\right|^2 = \frac{1}{a^2}\left[\frac{k}{2} + \frac{\gamma(\gamma-1)}{4k\tau^2} + \frac{3(\gamma-2)(\gamma-1)\gamma(\gamma+1)}{16k^3 \tau^4}\right], \quad (\text{A.7})$$

$$\left(\frac{v_k^{(2)}}{a}\right)'^2 = \frac{ke^{-2ik\tau}}{2a^2}\left(-1 + i\frac{\gamma(\gamma-1)}{k\tau} + \frac{\gamma(\gamma-1)(\gamma^2 - \gamma - 1)}{2k^2 \tau^2}\right), \quad (\text{A.8})$$

$$\left|\left(\frac{v_k^{(0)}(\tau)}{a}\right)'\right|^2 = \frac{1}{a^2}\frac{k}{2}, \quad (\text{A.9})$$

for the energy density.

$$|v_k^{(4)}(\tau)|^2 = \frac{1}{2k}\left[1 + \frac{\gamma(\gamma+1)}{2k^2 \tau^2} + \frac{3(\gamma+2)(\gamma+1)\gamma(\gamma-1)}{8k^4 \tau^4}\right], \quad (\text{A.10})$$

$$(v_k^{(2)}(\tau))^2 = \frac{e^{-2ik\tau}}{2k}\left(1 - i\frac{\gamma(\gamma+1)}{k\tau} - \frac{\gamma(\gamma+1)(\gamma^2 + \gamma - 1)}{2k^2 \tau^2}\right), \quad (\text{A.11})$$

$$|v_k^{(0)}(\tau)|^2 = \frac{1}{2k}, \quad (\text{A.12})$$

for the pressure. And

$$|v_k^{(2)}(\tau)|^2 = \frac{1}{2k} \left(1 + \frac{\gamma(\gamma+1)}{2k^2\tau^2} \right), \quad (\text{A.13})$$

$$(v_k^{(0)}(\tau))^2 = \frac{e^{-2ik\tau}}{2k}, \quad (\text{A.14})$$

for the power spectrum.

For inflation $a(\tau) \propto |\tau|^{\beta+1}$, just replacing $\gamma \rightarrow -\beta - 1$ in the above, one obtains the following adiabatic counter terms

$$\left| \left(\frac{v_k^{(4)}(\tau)}{a} \right)' \right|^2 = \frac{1}{a^2} \left[\frac{k}{2} + \frac{(\beta+1)(\beta+2)}{4k\tau^2} + \frac{3\beta(\beta+1)(\beta+2)(\beta+3)}{16k^3\tau^4} \right] \quad (\text{A.15})$$

for the energy density,

$$|v_k^{(4)}(\tau)|^2 = \frac{1}{2k} + \frac{\beta(\beta+1)}{4k^3\tau^2} + \frac{3(\beta-1)\beta(\beta+1)(\beta+2)}{16k^5\tau^4} \quad (\text{A.16})$$

for the pressure, and

$$\left| v_k^{(2)}(\tau) \right|^2 = \frac{1}{2k} + \frac{\beta(\beta+1)}{4k^3\tau^2} \quad (\text{A.17})$$

for the power spectrum.

B The solution mode at high frequency

It is revealing to expand the RGW mode solutions v_k at high frequency in terms of powers of k , in comparing with the adiabatic counter terms. For the present accelerating stage, the vacuum mode of RGW v_k in (6.5) at high frequencies can be expanded as powers of k as the following

$$\begin{aligned} v_k(\tau) = & \frac{e^{-ik\tau}}{\sqrt{2k}} \left(1 - i \frac{\gamma(\gamma+1)}{2k\tau} - \frac{(\gamma+2)(\gamma+1)\gamma(\gamma-1)}{8k^2\tau^2} \right. \\ & + i \frac{(\gamma+3)(\gamma+2)(\gamma+1)\gamma(\gamma-1)(\gamma-2)}{48k^3\tau^3} \\ & \left. + \frac{(\gamma+4)(\gamma+3)(\gamma+2)(\gamma+1)\gamma(\gamma-1)(\gamma-2)(\gamma-3)}{384k^4\tau^4} + \dots \right), \end{aligned} \quad (\text{B.1})$$

$$\begin{aligned} |v_k(\tau)|^2 = & \frac{1}{2k} \left[1 + \frac{\gamma(\gamma+1)}{2k^2\tau^2} + \frac{3(\gamma+2)(\gamma+1)\gamma(\gamma-1)}{8k^4\tau^4} \right. \\ & \left. + \frac{5(\gamma+3)(\gamma+2)(\gamma+1)\gamma(\gamma-1)(\gamma-2)}{16k^6\tau^6} + \dots \right], \end{aligned} \quad (\text{B.2})$$

$$\begin{aligned} v_k^2(\tau) = & \frac{e^{-2ik\tau}}{2k} \left(1 - i \frac{\gamma(\gamma+1)}{k\tau} - \frac{\gamma(\gamma+1)(\gamma^2+\gamma-1)}{2k^2\tau^2} \right. \\ & \left. + i \frac{(\gamma-1)\gamma(\gamma+1)(\gamma+2)(2\gamma^2+2\gamma-3)}{12k^3\tau^3} + \dots \right). \end{aligned} \quad (\text{B.3})$$

The derivatives are

$$\left(\frac{v_k}{a}\right)' = \frac{e^{-ik\tau}}{a\sqrt{2k}} \left(-ik - \frac{\gamma(\gamma-1)}{2\tau} + i\frac{(\gamma+1)\gamma(\gamma-1)(\gamma-2)}{8k\tau^2} + \frac{(\gamma+2)(\gamma+1)\gamma(\gamma-1)(\gamma-2)(\gamma-3)}{48k^2\tau^3} - i\frac{(\gamma+3)(\gamma+2)(\gamma+1)\gamma(\gamma-1)(\gamma-2)(\gamma-3)(\gamma-4)}{384k^3\tau^4} + \dots \right),$$

$$\left|\left(\frac{v_k}{a}\right)'\right|^2 = \frac{1}{a^2} \left[\frac{k}{2} + \frac{\gamma(\gamma-1)}{4k\tau^2} + \frac{3(\gamma-2)(\gamma-1)\gamma(\gamma+1)}{16k^3\tau^4} + \frac{5(\gamma-3)(\gamma-2)(\gamma-1)\gamma(\gamma+1)(\gamma+2)}{32k^5\tau^6} + \dots \right], \quad (\text{B.4})$$

$$\left(\left(\frac{v_k}{a}\right)'\right)^2 = \frac{e^{-2ik\tau}}{2a^2} k \left(-1 + i\frac{\gamma(\gamma-1)}{k\tau} + \frac{\gamma(\gamma-1)(\gamma^2-\gamma-1)}{2k^2\tau^2} - i\frac{(\gamma+1)\gamma(\gamma-1)(\gamma-2)(2\gamma^2-2\gamma-3)}{12k^3\tau^3} + \dots \right). \quad (\text{B.5})$$

For the inflation stage, the mode solution of RGW $v_k(\tau)$ of (2.13) at high frequencies can be expanded as the following

$$v_k(\tau) = \frac{e^{-ik\tau}}{\sqrt{2k}} \left(1 - i\frac{\beta(\beta+1)}{2k\tau} - \frac{(\beta+2)(\beta+1)\beta(\beta-1)}{8k^2\tau^2} + i\frac{(\beta+3)(\beta+2)(\beta+1)\beta(\beta-1)(\beta-2)}{48k^3\tau^3} + \frac{(\beta+4)(\beta+3)(\beta+2)(\beta+1)\beta(\beta-1)(\beta-2)(\beta-3)}{384k^4\tau^4} + \dots \right), \quad (\text{B.6})$$

where the first term is the Minkowski spacetime mode [the first term of (2.14)], and the remaining terms reflect the effect of the expanding RW spacetime. The squared absolute mode is

$$|v_k(\tau)|^2 = \frac{1}{2k} \left[1 + \frac{\beta(\beta+1)}{2k^2\tau^2} + \frac{3(\beta+2)(\beta+1)\beta(\beta-1)}{8k^4\tau^4} + \frac{5(\beta+3)(\beta+2)(\beta+1)\beta(\beta-1)(\beta-2)}{16(k\tau)^6} + \dots \right], \quad (\text{B.7})$$

where the first term $\frac{1}{2k}$ is the Minkowski spacetime vacuum term giving rise to $\Delta_t^2(k, \tau) \propto k^2$, and the second term $\frac{1}{2k} \frac{\beta(\beta+1)}{2k^2\tau^2}$ gives rise to $\Delta_t^2(k, \tau) \propto k^0$, respectively. The squared mode is

$$v_k(\tau)^2 = \frac{e^{-2ik\tau}}{2k} \left(1 - i\frac{\beta(\beta+1)}{k\tau} - \frac{(\beta+1)\beta(\beta^2+\beta-1)}{2k^2\tau^2} + i\frac{(\beta+2)(\beta+1)\beta(\beta-1)(2\beta^2+2\beta-3)}{12(k\tau)^3} + \dots \right). \quad (\text{B.8})$$

The time derivatives are given by

$$\begin{aligned} \left(\frac{v_k(\tau)}{a}\right)' &= \frac{1}{a} \frac{e^{-ik\tau}}{\sqrt{2k}} k \left(-\frac{i}{k\tau} - \frac{(\beta+1)(\beta+2)}{2k^2\tau^2} + i \frac{\beta(\beta+1)(\beta+2)(\beta+3)}{8k^3\tau^3} \right. \\ &\quad \left. + \frac{(\beta-1)\beta(\beta+1)(\beta+2)(\beta+3)(\beta+4)}{48k^4\tau^4} + \dots \right), \\ \left| \left(\frac{v_k(\tau)}{a}\right)' \right|^2 &= \frac{k}{2a^2} \left[1 + \frac{(\beta+1)(\beta+2)}{2k^2\tau^2} + \frac{3\beta(\beta+1)(\beta+2)(\beta+3)}{8k^4\tau^4} \right. \\ &\quad \left. + \frac{5(\beta-1)\beta(\beta+1)(\beta+2)(\beta+3)(\beta+4)}{16k^6\tau^6} + \dots \right], \end{aligned} \quad (\text{B.9})$$

$$\begin{aligned} \left(\left(\frac{v_k(\tau)}{a}\right)'\right)^2 &= \frac{e^{-2ik\tau}}{2a^2} k \left(-1 + i \frac{(\beta+1)(\beta+2)}{k\tau} + \frac{(\beta+1)(\beta+2)(\beta^2+3\beta+1)}{2k^2\tau^2} \right. \\ &\quad \left. - i \frac{\beta(\beta+1)(\beta+2)(\beta+3)(2\beta^2+6\beta+1)}{12k^3\tau^3} + \dots \right). \end{aligned} \quad (\text{B.10})$$

For de Sitter inflation, the exact expressions are obtained by letting $\beta+2=0$ in the asymptotic expressions (B.6)–(B.10). We emphasize that the above expressions (B.1)–(B.10) hold only for large k .

C Continuous Connection of Modes

Based on the Big-Bang cosmological model, the durations of four expansion stages after inflation are specified by the following: $\frac{a(\tau_H)}{a(\tau_E)} = 1.35$, $\frac{a(\tau_E)}{a(\tau_2)} = 2443.0$, $\frac{a(\tau_2)}{a(\tau_s)} = 10^{24}$, $\frac{a(\tau_s)}{a(\tau_1)} = 20$. See Ref. [9, 10] for details of the parameters of the scale factor, where the reheating duration $\frac{a(\tau_s)}{a(\tau_1)} = 300$ was used. $a(\tau)$ and $a'(\tau)$ have been chosen to be continuous at the joining points between adjoining two stages. From the observed CMB temperature $T_0 = 2.725\text{K}$ and the present Hubble constant $H_0 \simeq 2.13 h \times 10^{-42}\text{GeV}$ with $h \simeq 0.7$, this set of specification corresponds to $H \sim 3 \times 10^{14}\text{GeV}$ for inflation. Longer durations of reheating and radiation will lead to higher values of H .

The scale factor of inflation is given in (2.9). The mode during inflation by (2.12) and (2.13) is

$$u_k(\tau) = \sqrt{\frac{\pi}{2}} \sqrt{\frac{x}{2k}} \left[a_1 H_{\beta+\frac{1}{2}}^{(1)}(x) + a_2 H_{\beta+\frac{1}{2}}^{(2)}(x) \right], \quad -\infty < \tau \leq \tau_1, \quad (\text{C.1})$$

with $a_1 \equiv A_1 e^{i\pi(\beta+1)/2}$ and $a_2 \equiv A_2 e^{-i\pi(\beta+1)/2}$.

The scale factor for the reheating is

$$a(\tau) = a_z |\tau - \tau_p|^{1+\beta_s}, \quad \tau_1 < \tau < \tau_s$$

with $\beta_s \sim -0.7$. The mode during reheating is written as

$$u_k(\tau) = \sqrt{\frac{\pi}{2}} \sqrt{\frac{t}{2k}} \left[b_1 H_{\beta_s+\frac{1}{2}}^{(1)}(t) + b_2 H_{\beta_s+\frac{1}{2}}^{(2)}(t) \right], \quad (\text{C.2})$$

with $t \equiv k(\tau - \tau_p)$. By continuous connection of mode and its derivative at the end of inflation, $[u_k(\tau_1)]_{\text{inf}} = [u_k(\tau_1)]_{\text{reh}}$ and $[u'_k(\tau_1)]_{\text{inf}} = [u'_k(\tau_1)]_{\text{reh}}$, one gets

$$\begin{aligned}
b_1 = & -\frac{\pi}{4i} \frac{\sqrt{t_1}}{k} \left\{ \sqrt{\frac{x_1}{t_1}} \left(a_1 H_{\beta+\frac{1}{2}}^{(1)}(x_1) + a_2 H_{\beta+\frac{1}{2}}^{(2)}(x_1) \right) \left(\frac{k}{2\sqrt{t_1}} H_{\frac{1}{2}+\beta_s}^{(2)}(t_1) + \sqrt{t_1} H_{\frac{1}{2}+\beta_s}^{(2)'}(t_1) \right) \right. \\
& - H_{\frac{1}{2}+\beta_s}^{(2)}(t_1) \left[-\frac{k}{2x_1^{1/2}} \left(a_1 H_{\beta+\frac{1}{2}}^{(1)}(x_1) + a_2 H_{\beta+\frac{1}{2}}^{(2)}(x_1) \right) \right. \\
& \left. \left. + x_1^{1/2} \left(a_1 H_{\beta+\frac{1}{2}}^{(1)'}(x_1) + a_2 H_{\beta+\frac{1}{2}}^{(2)'}(x_1) \right) \right] \right\}, \tag{C.3}
\end{aligned}$$

$$\begin{aligned}
b_2 = & \frac{\pi}{4i} \frac{\sqrt{t_1}}{k} \left\{ \sqrt{\frac{x_1}{t_1}} \left(a_1 H_{\beta+\frac{1}{2}}^{(1)}(x_1) + a_2 H_{\beta+\frac{1}{2}}^{(2)}(x_1) \right) \left(\frac{k}{2\sqrt{t_1}} H_{\frac{1}{2}+\beta_s}^{(1)}(t_1) + \sqrt{t_1} H_{\frac{1}{2}+\beta_s}^{(1)'}(t_1) \right) \right. \\
& + H_{\frac{1}{2}+\beta_s}^{(1)}(t_1) \left[\frac{k}{2x_1^{1/2}} \left(a_1 H_{\beta+\frac{1}{2}}^{(1)}(x_1) + a_2 H_{\beta+\frac{1}{2}}^{(2)}(x_1) \right) \right. \\
& \left. \left. - x_1^{1/2} \left(a_1 H_{\beta+\frac{1}{2}}^{(1)'}(x_1) + a_2 H_{\beta+\frac{1}{2}}^{(2)'}(x_1) \right) \right] \right\}. \tag{C.4}
\end{aligned}$$

In the high frequency limit $k \rightarrow \infty$,

$$\begin{aligned}
b_1 = & e^{i(-x_1-t_1)+i\pi(\beta+\beta_s)/2} \left(-1 + i \frac{\beta(\beta+1)}{2x_1} + i \frac{\beta_s(\beta_s+1)}{2t_1} + \frac{\beta^2(\beta+1)^2}{8x_1^2} \right. \\
& \left. + \frac{\beta_s^2(\beta_s+1)^2}{8t_1^2} + \frac{\beta(\beta+1)\beta_s(\beta_s+1)}{4t_1x_1} \right) + \mathcal{O}(k^{-3}), \tag{C.5}
\end{aligned}$$

$$b_2 = e^{i(-x_1+t_1)+i\pi(\beta-\beta_s)/2} \left(\frac{\beta(\beta+1)}{4x_1^2} - \frac{\beta_s(\beta_s+1)}{4t_1^2} \right) + \mathcal{O}(k^{-3}). \tag{C.6}$$

During the radiation-dominant stage,

$$a(\tau) = a_e(\tau - \tau_e), \quad \tau_s \leq \tau \leq \tau_2, \tag{C.7}$$

and the mode function is

$$u_k(\tau) = \sqrt{\frac{\pi}{2}} \sqrt{\frac{y}{2k}} \left[c_1 H_{\frac{1}{2}}^{(1)}(y) + c_2 H_{\frac{1}{2}}^{(2)}(y) \right], \tag{C.8}$$

with $y \equiv k(\tau - \tau_e)$ and the coefficients as

$$\begin{aligned}
c_1 = & -\frac{\pi}{4i} \frac{\sqrt{y_s}}{k} \left\{ \sqrt{\frac{t_s}{y_s}} \left(b_1 H_{\beta_s+\frac{1}{2}}^{(1)}(t_s) + b_2 H_{\beta_s+\frac{1}{2}}^{(2)}(t_s) \right) \left(\frac{k}{2\sqrt{y_s}} H_{\frac{1}{2}}^{(2)}(y_s) + \sqrt{y_s} H_{\frac{1}{2}}^{(2)'}(y_s) \right) \right. \\
& - H_{\frac{1}{2}}^{(2)}(y_s) \left[\frac{k}{2t_s^{1/2}} \left(b_1 H_{\beta_s+\frac{1}{2}}^{(1)}(t_s) + b_2 H_{\beta_s+\frac{1}{2}}^{(2)}(t_s) \right) \right. \\
& \left. \left. + t_s^{1/2} \left(b_1 H_{\beta_s+\frac{1}{2}}^{(1)'}(t_s) + b_2 H_{\beta_s+\frac{1}{2}}^{(2)'}(t_s) \right) \right] \right\}, \tag{C.9}
\end{aligned}$$

$$\begin{aligned}
c_2 &= \frac{\pi \sqrt{y_s}}{4i k} \left\{ \sqrt{\frac{t_s}{y_s}} \left(b_1 H_{\beta_s + \frac{1}{2}}^{(1)}(t_s) + b_2 H_{\beta_s + \frac{1}{2}}^{(2)}(t_s) \right) \left(\frac{k}{2\sqrt{y_s}} H_{\frac{1}{2}}^{(1)}(y_s) + \sqrt{y_s} H_{\frac{1}{2}}^{(1)'}(y_s) \right) \right. \\
&\quad - H_{\frac{1}{2}}^{(1)}(y_s) \left[\frac{k}{2t_s^{1/2}} \left(b_1 H_{\beta_s + \frac{1}{2}}^{(1)}(t_s) + b_2 H_{\beta_s + \frac{1}{2}}^{(2)}(t_s) \right) \right. \\
&\quad \left. \left. + t_s^{1/2} \left(b_1 H_{\beta_s + \frac{1}{2}}^{(1)'}(t_s) + b_2 H_{\beta_s + \frac{1}{2}}^{(2)'}(t_s) \right) \right] \right\}, \tag{C.10}
\end{aligned}$$

where $t_s \equiv k(\tau_s - \tau_p)$ and $y_s \equiv k(\tau_s - \tau_e)$. In the limit $k \rightarrow \infty$

$$\begin{aligned}
c_1 &= e^{i(-x_1 - t_1 + t_s - y_s) + i\pi\beta/2} \left(-1 + i \frac{\beta(\beta+1)}{2x_1} + i \frac{\beta_s(\beta_s+1)}{2t_1} - i \frac{\beta_s(\beta_s+1)}{2t_s} \right. \\
&\quad + \frac{\beta^2(\beta+1)^2}{8x_1^2} + \frac{\beta_s^2(\beta_s+1)^2}{8t_1^2} + \frac{\beta_s^2(\beta_s+1)^2}{8t_s^2} + \frac{\beta(\beta+1)\beta_s(\beta_s+1)}{4t_1x_1} \\
&\quad \left. - \frac{\beta(\beta+1)\beta_s(\beta_s+1)}{4x_1t_s} - \frac{\beta_s^2(\beta_s+1)^2}{4t_1t_s} \right) + \mathcal{O}(k^{-3}), \tag{C.11}
\end{aligned}$$

$$\begin{aligned}
c_2 &= \left(\frac{\beta(\beta+1)}{4x_1^2} - \frac{\beta_s(\beta_s+1)}{4t_1^2} \right) e^{i(-x_1 + t_1 - t_s + y_s) + i\pi\beta/2} \\
&\quad + \frac{\beta_s(\beta_s+1)}{4t_s^2} e^{i(-x_1 - t_1 + t_s + y_s) + i\pi\beta/2} + \mathcal{O}(k^{-3}). \tag{C.12}
\end{aligned}$$

During the matter-dominant stage,

$$a(\tau) = a_m(\tau - \tau_m)^2, \quad \tau_2 \leq \tau \leq \tau_E, \tag{C.13}$$

and the mode function is

$$u_k(\tau) = \sqrt{\frac{\pi}{2}} \sqrt{\frac{z}{2k}} \left[d_1 H_{\frac{3}{2}}^{(1)}(z) + d_2 H_{\frac{3}{2}}^{(2)}(z) \right], \tag{C.14}$$

with $z \equiv k(\tau - \tau_m)$. The coefficients are

$$\begin{aligned}
d_1 &= -\frac{\pi \sqrt{z_2}}{4i k} \left\{ \sqrt{\frac{y_2}{z_2}} \left(c_1 H_{\frac{1}{2}}^{(1)}(y_2) + c_2 H_{\frac{1}{2}}^{(2)}(y_2) \right) \left(\frac{k}{2\sqrt{z_2}} H_{\frac{3}{2}}^{(2)}(z_2) + \sqrt{z_2} H_{\frac{3}{2}}^{(2)'}(z_2) \right) \right. \\
&\quad - H_{\frac{3}{2}}^{(2)}(z_2) \left[\frac{k}{2y_2^{1/2}} \left(c_1 H_{\frac{1}{2}}^{(1)}(y_2) + c_2 H_{\frac{1}{2}}^{(2)}(y_2) \right) \right. \\
&\quad \left. \left. + y_2^{1/2} \left(c_1 H_{\frac{1}{2}}^{(1)'}(y_2) + c_2 H_{\frac{1}{2}}^{(2)'}(y_2) \right) \right] \right\}, \tag{C.15}
\end{aligned}$$

$$\begin{aligned}
d_2 &= \frac{\pi \sqrt{z_2}}{4i k} \left\{ \sqrt{\frac{y_2}{z_2}} \left(c_1 H_{\frac{1}{2}}^{(1)}(y_2) + c_2 H_{\frac{1}{2}}^{(2)}(y_2) \right) \left(\frac{k}{2\sqrt{z_2}} H_{\frac{3}{2}}^{(1)}(z_2) + \sqrt{z_2} H_{\frac{3}{2}}^{(1)'}(z_2) \right) \right. \\
&\quad \left. - H_{\frac{3}{2}}^{(1)}(z_2) \left[\frac{k}{2y_2^{1/2}} \left(c_1 H_{\frac{1}{2}}^{(1)}(y_2) + c_2 H_{\frac{1}{2}}^{(2)}(y_2) \right) \right] \right\}
\end{aligned}$$

$$+y_2^{1/2} \left(c_1 H_{\frac{1}{2}}^{(1)'}(y_2) + c_2 H_{\frac{1}{2}}^{(2)'}(y_2) \right) \Big] \Big\}, \quad (\text{C.16})$$

where $y_2 \equiv k(\tau_2 - \tau_e)$ and $z_2 \equiv k(\tau_2 - \tau_m)$. In the limit $k \rightarrow \infty$,

$$\begin{aligned} d_1 = & i \left(-1 + i \frac{\beta(\beta+1)}{2x_1} + i \frac{\beta_s(\beta_s+1)}{2t_1} - i \frac{\beta_s(\beta_s+1)}{2t_s} + \frac{i}{z_2} + \frac{\beta^2(\beta+1)^2}{8x_1^2} \right. \\ & + \frac{\beta_s^2(\beta_s+1)^2}{8t_1^2} + \frac{\beta_s^2(\beta_s+1)^2}{8t_s^2} + \frac{1}{2z_2^2} + \frac{\beta(\beta+1)\beta_s(\beta_s+1)}{4x_1 t_1} \\ & - \frac{\beta(\beta+1)\beta_s(\beta_s+1)}{4x_1 t_s} + \frac{\beta(\beta+1)}{2x_1 z_2} - \frac{\beta_s^2(\beta_s+1)^2}{4t_1 t_s} + \frac{\beta_s(\beta_s+1)}{2t_1 z_2} \\ & \left. - \frac{\beta_s(\beta_s+1)}{2t_s z_2} \right) e^{i(-x_1-t_1+t_s-y_s+y_2-z_2)+i\pi\beta/2} + \mathcal{O}(k^{-3}), \end{aligned} \quad (\text{C.17})$$

$$\begin{aligned} d_2 = & i \left(-\frac{\beta(\beta+1)}{4x_1^2} + \frac{\beta_s(\beta_s+1)}{4t_1^2} \right) e^{i(-x_1+t_1-t_s+y_s-y_2+z_2)+i\pi\beta/2} \\ & - i \frac{\beta_s(\beta_s+1)}{4t_s^2} e^{i(-x_1-t_1+t_s+y_s-y_2+z_2)+i\pi\beta/2} \\ & + \frac{i}{2z_2^2} e^{i(-x_1-t_1+t_s-y_s+y_2+z_2)+i\pi\beta/2} + \mathcal{O}(k^{-3}). \end{aligned} \quad (\text{C.18})$$

The present accelerating stage has

$$a(\tau) = l_H |\tau - \tau_a|^{-\gamma}, \quad \tau_E \leq \tau \leq \tau_H, \quad (\text{C.19})$$

with $\gamma \simeq 2.108$, fits the model $\Omega_\Lambda \simeq 0.7$ and $\Omega_m = 1 - \Omega_\Lambda$. The normalization of $a(\tau)$ is taken such that $|\tau_H - \tau_a| = 1$ and $a(\tau_H) = l_H$. The present Hubble constant is $H_0 = (a'/a^2)|_{\tau_H} = \gamma l_H^{-1}$. The mode function is

$$u_k(\tau) = \sqrt{\frac{\pi}{2}} \sqrt{\frac{s}{2k}} \left[e^{-i\pi\gamma/2} \beta_k H_{-\gamma-\frac{1}{2}}^{(1)}(s) + e^{i\pi\gamma/2} \alpha_k H_{-\gamma-\frac{1}{2}}^{(2)}(s) \right], \quad (\text{C.20})$$

with $s \equiv k|\tau - \tau_a| = -k(\tau - \tau_a)$ and

$$\begin{aligned} e^{-i\pi\gamma/2} \beta_k = & \frac{\pi \sqrt{s_E}}{4i k} \left\{ \sqrt{\frac{z_E}{s_E}} \left(d_1 H_{\frac{3}{2}}^{(1)}(z_E) + d_2 H_{\frac{3}{2}}^{(2)}(z_E) \right) \left(-\frac{k}{2z_E^{1/2}} H_{-\gamma-\frac{1}{2}}^{(2)}(s_E) + z_E^{1/2} H_{-\gamma-\frac{1}{2}}^{(2)'}(s_E) \right) \right. \\ & - H_{-\gamma-\frac{1}{2}}^{(2)}(s_E) \left[\frac{k}{2z_E^{1/2}} \left(d_1 H_{\frac{3}{2}}^{(1)}(z_E) + d_2 H_{\frac{3}{2}}^{(2)}(z_E) \right) \right. \\ & \left. \left. + z_E^{1/2} \left(d_1 H_{\frac{3}{2}}^{(1)'}(z_E) + d_2 H_{\frac{3}{2}}^{(2)'}(z_E) \right) \right] \right\}, \end{aligned} \quad (\text{C.21})$$

$$\begin{aligned} e^{i\pi\gamma/2} \alpha_k = & \frac{\pi \sqrt{s_E}}{4i k} \left\{ \sqrt{\frac{z_E}{s_E}} \left(d_1 H_{\frac{3}{2}}^{(1)}(z_E) + d_2 H_{\frac{3}{2}}^{(2)}(z_E) \right) \left(\frac{k}{2z_E^{1/2}} H_{-\gamma-\frac{1}{2}}^{(1)}(s_E) - z_E^{1/2} H_{-\gamma-\frac{1}{2}}^{(1)'}(s_E) \right) \right. \\ & \left. + H_{-\gamma-\frac{1}{2}}^{(1)}(s_E) \left[\frac{k}{2z_E^{1/2}} \left(d_1 H_{\frac{3}{2}}^{(1)}(z_E) + d_2 H_{\frac{3}{2}}^{(2)}(z_E) \right) \right] \right\} \end{aligned}$$

$$+z_E^{1/2} \left(d_1 H_{\frac{3}{2}}^{(1)'}(z_E) + d_2 H_{\frac{3}{2}}^{(2)'}(z_E) \right) \Big] \Big\}, \quad (\text{C.22})$$

where $z_E \equiv k(\tau_E - \tau_m)$ and $s_E \equiv -k(\tau_E - \tau_a)$. In the limit $k \rightarrow \infty$, the expansion of β_k and α_k are given by (6.2) (6.3).

References

- [1] R.P. Feynman, A.R. Hibbs, *Quantum mechanics and path integration*, McGraw-Hill, (1965)
- [2] L. H. Ford and L. Parker, Quantized gravitational wave perturbations in Robertson-Walker universes, *Phys. Rev. D* **16**, 1601 (1977).
- [3] A. A. Starobinsky, Relic gravitation radiation spectrum and initial state of the universe, *JETP Lett.* **30**, 682(1979).
- [4] B. Allen, Stochastic gravity-wave background in inflationary-universe models, *Phys. Rev. D* **37**, 2078 (1988).
- [5] L. P. Grishchuk, The implications of microwave background anisotropies for laser-interferometer-tested gravitational waves, *Class. Quantum Grav.* **14** 1445 (1997).
- [6] L. P. Grishchuk, Relic gravitational waves and their detection, *Lect. Notes Phys.* **562** 167, (2001); arXiv:gr-qc/0002035.
- [7] M. Giovannini, *Phys. Rev. D* **60**, 123511 (1999).
- [8] B. Allen and J.D. Romano, Detecting a stochastic background of gravitational radiation: Signal processing strategies and sensitivities, *Phys. Rev. D* **59**, 102001 (1999).
- [9] Y. Zhang, *et al.*, Relic gravitational waves in the accelerating Universe, *Class. Quantum Grav.* **22**, 1383 (2005).
- [10] Y. Zhang, *et al.*, An exact analytic spectrum of relic gravitational waves in an accelerating universe, *Class. Quantum Grav.* **23**, 3783 (2006).
- [11] F.Y. Li, M. X. Tang, D. P. Shi, Electromagnetic response of a Gaussian beam to high-frequency relic gravitational waves in quintessential inflationary models, *Phys. Rev. D* **67**, 104008 (2003).
- [12] M. L. Tong, Y. Zhang, and F. Y. Li, Using a polarized maser to detect high-frequency relic gravitational waves, *Phys.Rev. D* **78**, 024041 (2008).
- [13] L. Parker and S.A. Fulling, Adiabatic regularization of the energy-momentum tensor of a quantized field in homogeneous spaces, *Phys. Rev. D* **9**, 341 (1974).
- [14] S. A. Fulling, L. Parker, B. L. Hu, Conformal energy-momentum tensor in curved spacetime: Adiabatic regularization and renormalization, *Phys. Rev. D* **10**, 3905 (1974).
- [15] T. S. Bunch, Adiabatic regularisation for scalar fields with arbitrary coupling to the scalar curvature, *J. Phys. A* **13**, 1297 (1980).

- [16] P. R. Anderson and L. Parker, Adiabatic regularization in closed Robertson-Walker universes, *Phys. Rev. D* **36**, 2963 (1987).
- [17] N. D. Birrell and P. C. W. Davies, *Quantum Fields in Curved Space* (Cambridge University Press, Cambridge, England, 1982).
- [18] L. Parker and D. J. Toms, *Quantum Field Theory in Curved Spacetime: Quantized Fields and Gravity* (Cambridge University Press, Cambridge, England, 2009).
- [19] I. Agullo, J. Navarro-Salas, G. J. Olmo, L. Parker, Reexamination of the power spectrum in de Sitter inflation *Phys. Rev. Lett.* **101**, 171301 (2008).
- [20] R. Durrer, G. Marozzi and M. Rinaldi, Adiabatic renormalization of inflationary perturbations *Phys. Rev. D* **80**, 065024 (2009).
- [21] G. Marozzi M. Rinaldi and R. Durrer, On infrared and ultraviolet divergences of cosmological perturbations *Phys. Rev. D* **83**, 105017 (2011).
- [22] Y. Urakawaa and A. A. Starobinsky, Adiabatic regularization of primordial perturbations generated during inflation, Proceedings of 19th Workshop in General Relativity and Gravitation in Japan (JGRG19), Tokyo Japan (2009), pg. 367, <http://www2.rikkyo.ac.jp/web/jgrg19/Proceedings/pdf/O25.pdf>
- [23] A. L. Alinea, T. Kubota, Y. Nakanishia, W. Naylor, Adiabatic regularisation of power spectra in k-inflation *JCAP* 06, 019 (2015)
- [24] A. L. Alinea, Adiabatic regularization of power spectra in nonminimally coupled chaotic inflation, *JCAP* 10, 027 (2016).
- [25] A. L. Alinea and T. Kubota, Adiabatic regularization of the power spectrum in nonminimally coupled general single-field inflation *Phys. Rev. D* **97**, 063513 (2018)
- [26] T. Markkanen, Renormalization of the inflationary perturbations revisited, *JCAP* 05, 001 (2018).
- [27] T. Markkanen and A. Tranberg, A simple method for one-loop renormalization in curved space-time, *JCAP* 08, 045 (2013).
- [28] D.G. Wang, Y. Zhang, and J.W. Chen, Vacuum and Gravitons of Relic Gravitational Waves, and Regularization of Spectrum and Energy-Momentum Tensor, *Phys.Rev D* **94**, 044033 (2016).
- [29] W. Zhao and Y. Zhang, An Analytic Approach to CMB Polarizations Generated by Relic Gravitational Waves, *Phys. Rev. D* **74**, 083006 (2006).
- [30] T. Y. Xia and Y. Zhang, Analytic Spectra of CMB Anisotropies and Polarization Generated by Relic Gravitational Waves with Modification due to Neutrino Free-Streaming, *Phys. Rev. D* **78**, 123005 (2008);
- [31] T. Y. Xia and Y. Zhang, Approximate Analytic Spectra of Reionized CMB Anisotropies and Polarization generated by Relic Gravitational Waves, *Phys. Rev. D* **79** 083002 (2009);

- [32] Z. Cai and Y. Zhang, Analytic Spectra of CMB Anisotropies and Polarization Generated by Scalar Perturbations in Synchronous Gauge, *Class. Quant. Grav.* **29**, 105009 (2012).
- [33] B. Wang and Y. Zhang, Second-order cosmological perturbations. I. Produced by scalar-scalar coupling in synchronous gauge, *Phys.Rev .D* **98**, 103522, (2017).
- [34] Y. Zhang, F. Qin, and B. Wang, Second-order cosmological perturbations. II. Produced by scalar-tensor and tensor-tensor couplings, *Phys.Rev .D* **98**, 103523, (2017).
- [35] E. Komatsu, et al, Seven-Year Wilkinson Microwave Anisotropy Probe (WMAP) Observations: Cosmological Interpretation, *Astrophys. J. Suppl.***192**, 18 (2011).
- [36] G. Hinshaw, et al., Nine-year Wilkinson Microwave Anisotropy Probe (WMAP) observations: cosmological parameter results, *Astrophys. J. Suppl.* **208**, 19 (2013)
- [37] A. Kosowsky and M. S. Turner, CBR anisotropy and the running of the scalar spectral index, *Phys. Rev. D* **52**, R1739 (1995).
- [38] N. D. Spergel, et al, First-year Wilkinson Microwave Anisotropy Probe (WMAP) observations: determination of cosmological parameters, *Astrophys. J. Suppl.* **148**, 175 (2003).
- [39] H. V. Peiris, et al, First Year Wilkinson Microwave Anisotropy Probe (WMAP) Observations: Implications for Inflation, *Astrophys. J. Suppl.* **148**, 213 (2003).
- [40] S. Weinberg, *Gravitation and Cosmology*, John Wiley, (1972).
- [41] R. A. Isaacson, Gravitational radiation in the limit of high frequency. I. The linear approximation and geometrical optics, *Phys. Rev.* **166**, 1263 (1968).
- [42] R. A. Isaacson, Gravitational radiation in the limit of high frequency. II. Nonlinear terms and the effective stress tensor, *Phys. Rev.* **166**, 1272 (1968).
- [43] D.R. Brill and J.B. Hartle, Method of the self-consistent field in general relativity and its application to the gravitational geon, *Phys. Rev.* **135**, B271 (1964).
- [44] D.Q. Su and Y. Zhang, Energy-momentum pseudotensor of relic gravitational waves in an expanding universe, *Phys. Rev. D* **85**, 104012 (2012).
- [45] L.R. Abramo, R.H. Brandenberger, and V.F. Mukhanov, Energy-momentum tensor for cosmological perturbations, *Phys. Rev. D* **56** 3248 (1997).
- [46] V. Sahni, Energy density of relic gravity waves from inflation, *Phys. Rev. D* **42**, 453 (1990).
- [47] M. Giovannini, Dynamical backreaction of relic gravitons, *Phys.Rev.D* **73**, 083505 (2006).
- [48] L. H. Ford, Quantum instability of de Sitter spacetime, *Phys. Rev. D* **31**, 701 (1985).
- [49] A. Lewis, A. Challinor, and A. Lasenby, Efficient computation of cosmic microwave background anisotropies in closed Friedmann-Robertson-Walker models, *Astrophys. J.* **538**, 473 (2000).

- [50] A. Lewis and A. Challinor, <http://camb.info/>
- [51] U. Seljak and M. Zaldarriaga, A line of sight approach to cosmic microwave background anisotropies, *Astrophys. J.* **469**, 437 (1996).
- [52] R. Smits, et al, Pulsar searches and timing with the square kilometre array, *A&A* **493**, 1161 (2009).
- [53] <https://www.skatelescope.org/project/>
- [54] R. van Haasteren, et al, Placing limits on the stochastic gravitational-wave background using European Pulsar Timing Array data, *Mon. Not. R. Astron. Soc.* **414**, 3117 (2011).
- [55] R. Nan, et al, The five-hundred-meter aperture spherical radio telescope (FAST) project, *Int. J. Mod. Phys. D* **20**, 989 (2011).
- [56] P.B. Demorest et al, Limits on the stochastic gravitational wave background from the North American nanohertz observatory for gravitational waves, *Astrophys. J.* **762** 94 (2013).
- [57] M. L. Tong *et al.*, Using pulsar timing arrays and the quantum normalization condition to constrain relic gravitational waves, *Class. Quantum Grav.* **31**, 035001 (2014).
- [58] <http://lisa.nasa.gov/>
- [59] <http://sci.esa.int/lisa/>
- [60] <https://www.ligo.org/index.php>
- [61] M. Sasaki, Large scale quantum fluctuations in the inflationary universe, *Prog. Theor. Phys.* **76**, 1036 (1986).
- [62] J.-c. Hwang, Curved space quantum scalar field theory with accompanying metric fluctuations, *Phys. Rev. D* **48**, 3544 (1993).
- [63] J.-c. Hwang, Cosmological Perturbations with Multiple Scalar Fields, arXiv:gr-qc/9608018.
- [64] C. Gordon, D. Wands, B. A. Bassett and R. Maartens, Adiabatic and entropy perturbations from inflation, *Phys. Rev. D* **63**, 023506 (2000).
- [65] B. Chakraborty, The mathematical problem of reflection solved by an extension of the WKB method, *J. Math. Phys.* **14**, 188 (1973).